Open Access

SCHOLARENA

Journal of Nanoscience and Nanotechnology Applications

REVIEW ARTICLE

ISSN: 2577-7920

Aurora-Inspired Optimization: A Novel Approach for Precise Parameter Estimation in Proton Exchange Membrane Fuel Cells

Mohsen Abdollahzadeh Aghbolagh[*]

School of Information Technology and Data Science, Irkutsk National Research Technical University, Irkutsk, 664074, Russia

[*]**Corresponding Author:** Mohsen Abdollahzadeh Aghbolagh, School of Information Technology and Data Science, Irkutsk National Research Technical University, Irkutsk, 664074, Russia, Tel.: 89149351170, E-mail: mohsen@istu.edu

Citation: Mohsen Abdollahzadeh Aghbolagh (2024) Aurora-Inspired Optimization: A Novel Approach for Precise Parameter Estimation in Proton Exchange Membrane Fuel Cells, J Nanosci Nanotechnol Appl 9: 101

Abstract

Proton Exchange Membrane Fuel Cells (PEMFCs) are vital components of sustainable energy systems due to their high efficiency and environmentally friendly energy conversion. However, the complex nonlinear behavior of PEMFC models presents significant challenges for parameter estimation, affecting both operational reliability and longevity. This study introduces the Aurora-Inspired Optimization (AIO) algorithm, which leverages principles derived from auroral phenomena to enhance parameter estimation accuracy. AIO employs aurora gyration motion for refined local search and aurora oval walk for efficient global exploration, ensuring an optimal balance between exploration and exploitation. The algorithm's effectiveness is benchmarked against established optimization methods—including GSA, DE, PSO, MFO, ACOR, MVO, WOA, SCA, and JAYA—across six PEMFC models: BCS 500 W, Nedstack 600 W PS6, SR-12 W, Horizon H-12, Ballard Mark V, and STD 250 W Stack. Results demonstrate that AIO surpasses competing algorithms by achieving the lowest Sum of Squared Errors (SSE) and the fastest convergence rates. Specifically, SSE values of 0.025493 for the BCS 500 W model, 0.275211 for the Nedstack 600 W PS6, and 0.283774 for the STD 250 W Stack are observed, alongside minimal Absolute Error (AE) and Relative Error (RE%), such as AE = 0.259293 and RE% = 1.185075 for the STD 250 W Stack. Additionally, AIO consistently stabilizes within 50 iterations across all test cases and achieves the highest Friedman Ranking score of 1. These findings highlight the potential of AIO to significantly enhance predictive accuracy, operational reliability, and energy output in PEMFC systems, establishing it as a powerful tool for fuel cell optimization. Faster convergence and lower runtime are critical in real-time control and adaptive systems, where quick parameter tuning enhances system responsiveness and energy efficiency, particularly in dynamic environments such as electric vehicles or grid-connected fuel cells.

Keywords: Metaheuristic Optimization; Parameter Estimation; Polar Lights Optimization (PLO); Proton Exchange Membrane Fuel Cells (PEMFCs); Sum of Squared Errors (SSE)

Introduction

In disciplines such as engineering and economics, optimization and intelligent algorithms play a pivotal role in enhancing model performance and accuracy. In recent years, there has been a growing integration of deep learning techniques with optimization methods to address complex problem domains. This synergy facilitates the development of precise and efficient solutions that often surpass the capabilities of conventional approaches. For example, deep learning models have proven effective in domains such as sentiment analysis, structural health monitoring, and medical diagnostics.

Despite these advancements, certain fields—particularly energy systems—present distinct challenges that necessitate the development of novel methodological approaches. Proton Exchange Membrane Fuel Cells (PEMFCs), a promising form of fuel cell technology, have emerged as sustainable energy solutions within this context. Due to their high efficiency and environmentally friendly operation, PEMFCs are particularly suitable for renewable energy applications. However, accurately modeling these systems and estimating their parameters remain significant challenges, primarily due to their nonlinear behavior and multivariable interactions. Optimal performance, accurate lifespan prediction, and operational reliability of PEMFCs hinge on the precise estimation of their parameters.

The global push toward decarbonization has accelerated the adoption of fuel cells, including PEMFCs, in the power generation and transportation sectors. Their high efficiency, zero-emission operation, and potential to replace fossil fuels in heavy-duty applications—such as trucking and maritime transport—make them especially appealing. Nonetheless, several critical challenges hinder their widespread deployment:

1. Complex Modeling Requirements: PEMFCs exhibit nonlinear interdependencies among chemical, thermal, and electrical processes, complicating accurate modeling and optimization.

2. Parameter Estimation Difficulties: The seven essential parameters that govern PEMFC performance are typically not disclosed in manufacturers' specifications, necessitating empirical optimization techniques.

3. Lifespan and Reliability Issues: Performance degradation over time highlights the importance of developing accurate and predictive models to ensure long-term reliability. Overcoming these challenges requires the implementation of robust optimization algorithms that can effectively manage the trade-off between local exploitation and global exploration, while ensuring convergence to globally optimal solutions.

Previous Work and Contributions

Over the past decade, numerous optimization algorithms have been explored for enhancing the modeling and parameter estimation of Proton Exchange Membrane Fuel Cells (PEMFCs). Metaheuristic approaches, such as Whale Optimization [2], Chicken Swarm Optimization [12], Slime Mold Algorithm [13], and Bald Eagle Search [14], have shown potential in nonlinear systems but often lack dynamic validation or scalability. Extensions specific to PEMFCs—e.g., differential evolution [7], multi--objective models [6], and hybrid techniques [20]—have improved estimation accuracy but frequently omit real-world deployment or long-term degradation effects.

Studies focusing on system behavior and modeling—such as adaptive control [15], environmental variability [8], and dynamic estimation frameworks [21,30]—have addressed isolated aspects but seldom offer a comprehensive solution. Others have proposed neural networks [37], advanced controllers [22], and algorithmic refinements [23,24], yet many approaches suffer from premature convergence, inadequate exploration, or computational inefficiency. Additionally, practical frameworks [1,28] and real-time strategies [29,31] remain underexplored in dynamic, scalable applications.

Despite substantial progress, key challenges persist: weak adaptability to dynamic conditions, insufficient real-world validation, and limited exploration–exploitation balance during optimization. These limitations hinder robust, scalable modeling essential for reliable PEMFC integration into smart energy systems.

To address these gaps, this study introduces the Polar Lights Optimization (PLO) algorithm—an innovative, nature-inspired framework designed for precise, efficient, and scalable PEMFC parameter estimation. The key contributions are as follows:

1. Novel Algorithmic Design: PLO mimics auroral dynamics via gyration motion (local exploitation) and aurora oval walk (global exploration), achieving balanced, adaptive optimization.

2. Robust Validation: The algorithm is tested across six distinct PEMFC models, demonstrating wide applicability and model versatility.

3. Superior Performance: Benchmarking against nine leading algorithms confirms PLO's advantage in convergence speed, modeling precision, and error minimization.

4. Real-World Relevance: PLO's outputs enhance I-V curve alignment, support real-time modeling, and promote scalable deployment in renewable energy systems.

5. Strategic Impact: By bridging theoretical advancements with practical applicability, this work advances the integration of PEMFCs in future-ready energy infrastructures.

The remainder of the paper is organized as follows

Motivation for Aurora Dynamics in PEMFC Optimization

PEMFCs are a type of fuel cell that convert chemical energy directly into electrical energy through an electrochemical reaction between hydrogen and oxygen. They operate at low temperatures (typically below 100°C), are compact, efficient, and emit only water as a byproduct, making them well-suited for portable, stationary, and vehicular applications. The dynamic behavior of Aurora phenomena—characterized by gyration motion (localized turbulence) and oval walking (global path following)—mirrors the complexity of PEMFC parameter spaces, which are highly nonlinear and exhibit multiple local optima. These natural dynamics offer an intuitive framework for balancing exploration (searching broadly across the solution space) and exploitation (refining known good regions).

As a result, aurora-inspired motion provides a powerful analogy and mechanism for navigating the rugged parameter landscape of PEMFCs, making it particularly well-suited for robust, adaptive parameter estimation.

PEMFC Mathematical Modelling

Basic Concept of PEMFC

A Proton Exchange Membrane Fuel Cell (PEMFC) consists of two electrodes—the anode and the cathode—separated by a proton-conducting membrane, which serves as the polymer electrolyte.

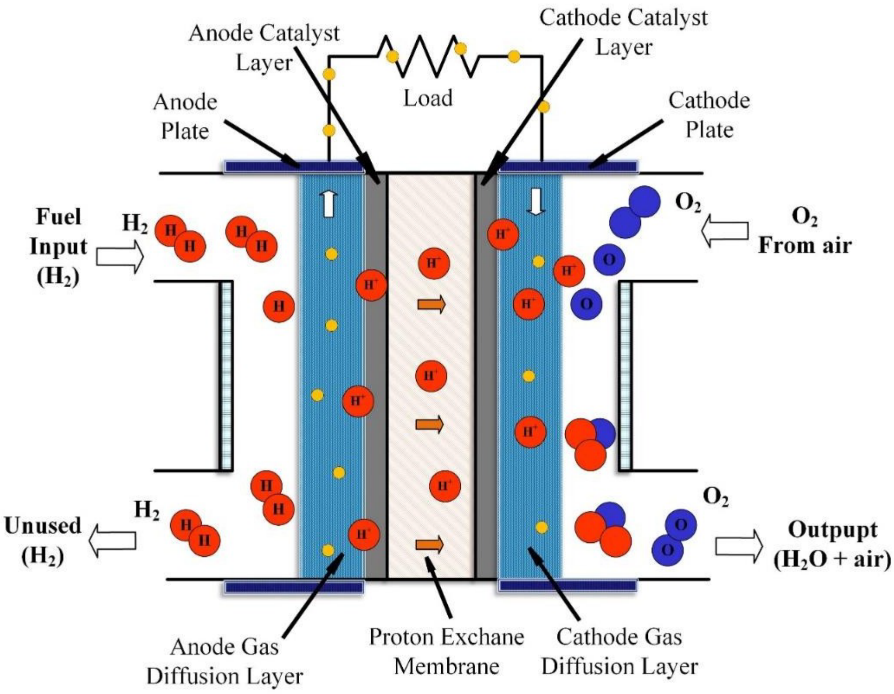

Figure 1: Schematic Diagram for Fuel Cell

This configuration allows protons to pass through the membrane while preventing electron flow, ensuring the proper functioning of the electrochemical process [36]. Catalyst layers are placed between the electrolyte membrane and both electrodes to accelerate chemical reactions.

At the anode, hydrogen gas undergoes dissociation at the catalyst layer, splitting into protons and electrons. The protons migrate through the membrane toward the cathode, while the electrons travel through an external circuit, generating electricity. Simultaneously, oxygen (or air) is supplied to the cathode, where it reacts with the incoming protons and returning electrons, forming water. The fundamental electrochemical reactions occurring in PEMFCs are:

Anode reaction (1) and Cathode reaction (2)

$$\mathrm{H_2} \rightarrow 2\mathrm{H}^+ + 2\mathrm{e}^- \quad (1)$$

$$2H^+ + \frac{1}{2}O_2 \rightarrow H_2O \quad (2)$$

Overall reaction:

$$H_2 + \frac{1}{2}O_2 \rightarrow H_2O + \mathrm{Energy} + \mathrm{Heat} \quad (3)$$

In the overall reaction, “Energy” represents the electrical power generated as electrons flow from the anode to the cathode through the external circuit. The equivalent electrical circuit for a PEMFC stack is depicted in Figure 2.

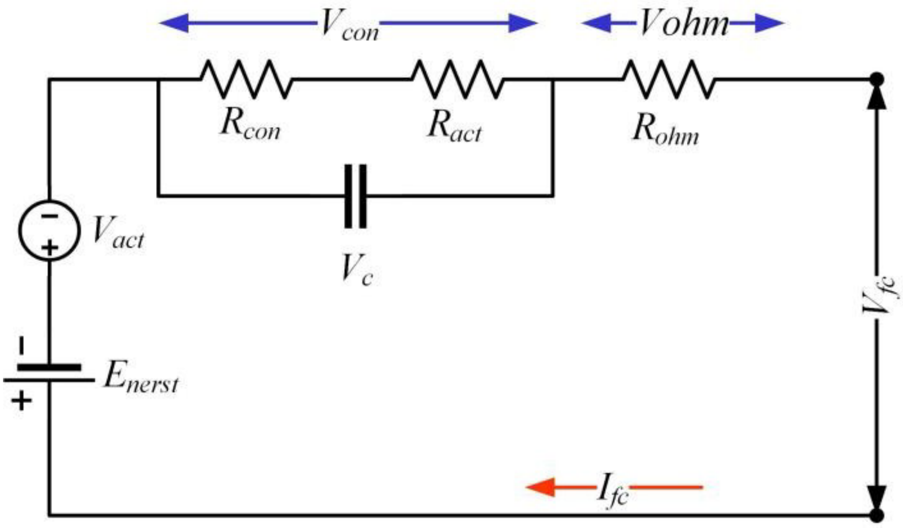

Figure 2: PEMFC Equivalent Circuit

Mathematical Model of PEMFC Stacks

The voltage output of a single fuel cell, denoted as V_{cell}, can be expressed using the following equation:

$$\Delta V_{cell} = \Delta E_{nerst} - \Delta V_{act} - \Delta V_{ohm} - \Delta V_{con} \quad (4)$$

Where, E_{nerst} represents the open-circuit voltage of the cell also known as the Nernst potential, ΔVact accounts for activation losses, which occur due to the energy required for electrochemical reactions, ΔV_{ohm} represents the ohmic losses, arising from resistance in the membrane and electrical pathways, and ΔV_{con} corresponds to concentration losses, which result from limitations in mass transport as the reactants are consumed. A fuel cell stack, which consists of multiple fuel cells connected in series to increase the voltage, has an overall stack voltage defined by:

Open-Circuit Voltage (Reversible Potential) Calculation

Here, N_{cells} refers to the number of cells connected in series, and Vcell is the output voltage for each individual fuel cell, as derived from Equation (4).

The reversible potential, E_{nerst}, is calculated as follows [11, 12]:

Where T_{fc} is the cell absolute operating temperature in Kelvin, while P_{H_2} and P_{0_2} denote the partial pressures of hydrogen and oxygen in the fuel cell stack input channels (atm). When hydrogen and air serve as the inputs, the partial oxygen pressure, P_{0_2}, is determined as follows [13, 14]:

$$P_{O_2} = P_c - RH_c P_{H_2O}^{sat} - \frac{0.79}{0.21} P_{O_2} \cdot \exp\left(0.291 \frac{I_{fc}}{A} / T_{fc}^{0.832}\right) \quad (7)$$

Here P_c represents the inlet channel pressure at the cathode (atm), RH_c is the cathode electrode relative humidity, I_{fc} is the operating current (A), A is the membrane surface area (cm²), and $P_{H_2O}^{sat}$ is the water vapor pressure at saturation, defined by [15]:

$$\log_{10}(P^{sat})_{H_20} = 2.95\times10^{-2}(T_{fc}-273.15) - 9.18\times10^{-5}(T_{fc}-273.15)^2 + 1.44\times10^{-7}(T_{fc}-273.15)^3 - 2.18 (8)$$

In cases where hydrogen and pure oxygen are used, the partial oxygen pressure P_{0_2} is calculated as follows [15]:

$$P_{O_2} = RH_c P_{H_2O}^{sat}\left[\left(\exp\left(4.192 \frac{1}{I_{fc}} / T_{fc}^{1.334}\right) \cdot \frac{RH_c P_{H_2O}^{sat}}{P_a}\right)^{-1} - 1\right] \quad (9)$$

In both cases, the partial hydrogen pressure P_{H_2} is given by:

$$P_{H_2} = 0.5RH_a P_{H_2O}^{sat}\left[\left(\exp\left(1.635\frac{1}{I_{fc}}/T_{fc}^{1.334}\right)\cdot\frac{RH_a P_{H_2O}^{sat}}{P_a}\right)^{-1} - 1\right] \quad (10)$$

Where P_a is the anode electrode inlet channel pressure (atm), and RH_a represents the relative humidity on the anode side.

The activation voltage drop ΔV_{act} for the electrodes is calculated by:

$$\Delta V_{act} = -[\xi_1 + \xi_2 T_{fc} + \xi_3 T_{fc} ln(C_{O_2}) + \xi_4 T_{fc} ln(I_{fc})] \quad (11)$$

Where $\xi 1, \xi 2, \xi 3$ and $\xi 4$ are empirical coefficients, while C_{O_2} denotes the oxygen concentration at the cathode (mol/cm³) as follows:

$$C_{O_2} = \frac{P_{O_2}}{5.08\times 10^6 \cdot \exp\left(-498/f_{fc}\right)} \quad (12)$$

The ohmic overpotential, ΔV_{ohm} accounts for resistance within the fuel cell and is calculated using:

$$\Delta V_{\text{ohm}} = I_{fc}(R_M + R_C) \quad (13)$$

R_M is the membrane resistance (Ω) and R_C is the resistance due to proton movement through the membrane. Membrane resistance is calculated as:

$$R_M = \frac{\rho_M \cdot l}{A} \quad (14)$$

Where ρ_M represents specific membrane resistance (Ω·cm), representing membrane thickness (cm), and the empirical formula for ρ_M given as:

$$\rho_M = \frac{181.6\left[1 + 0.03\left(\frac{I_{fc}}{A}\right) + 0.062\left(\frac{T_{fc}}{303}\right)^2\left(\frac{I_{fc}}{A}\right)^{2.5}\right]}{\left[\lambda - 0.634 - 3\left(\frac{I_{fc}}{A}\right)\right]\times\exp\left[4.18\left(\frac{T_{fc}-303}{T_{fc}}\right)\right]} \quad (15)$$

λ is an adjustable parameter connected to membrane preparation.

The concentration voltage drop, ΔV_{con}, is determined by:

$$\Delta V_{\text{con}} = -b\ln\left(1 - \frac{J}{J_{\text{max}}}\right) \quad (16)$$

Where b is a fitting parameter (V); J and J_{max} are the operating current density and maximum current density (A/cm²), respectively.

To ensure accurate modeling and simulation seven unknown parameters (ξ_1, ξ_2, ξ_3, ξ_4, λ, R_C, and b) must be estimated. The proposed Polar Lights Optimization (PLO) algorithm is employed to optimize these parameters for improved PEMFC performance and accuracy.

Objective Function

To ensure the modeled PEMFC output aligns closely with empirical data, the optimization problem is formulated by minimizing the Sum of Squared Errors (SSE) between the experimentally recorded stack voltages and the model-predicted values, using the following expression [16, 17]:

$$\text{OF} = \min \text{SSE}(x) = \min \sum_{i=1}^{N}\left[v_{\text{meas}}(i) - v_{\text{cal}}(i)\right]^2 \quad (17)$$

Where: x is the vector of unknown parameters to be optimized, N denotes the total number of data points, i is the iteration index, v_{meas} and v_{cal} represent the measured and calculated voltages. The optimization process is subject to the following boundary constraints:

$$\begin{aligned} &\xi_{i,\min} \leqslant \xi_i \leqslant \xi_{i,\max}, i = 1:4 \qquad (18) \\ &R_{c,\min} \leqslant R_c \leqslant R_{c,\max} \\ &\lambda_{\min} \leqslant \lambda \leqslant \lambda_{\max} \\ &b_{\min} \leqslant b \leqslant b_{\max} \end{aligned}$$

Where $\xi_{i,min}$ and $\xi_{i,\ max}$ define permissible ranges for the empirical coefficients, $R_{C,min}$ and $R_{C,max}$ are resistance bounds, and $\lambda_{\min}$,$\lambda_{\max}$ $b$min, and $b$max define the limits for water content and parametric coefficients. The Mean Bias Error (MBE) is employed as an additional performance metric, calculated as:

$$\mathrm{MBE} = \frac{\sum_{i=1}^{N} |V_{\mathrm{meas}}(i) - V_{\mathrm{calc}}(i)|}{N} \quad (19)$$

PLO Algorithm Methodology

This section elaborates the Polar Lights Optimization (PLO) algorithm, an optimization strategy inspired by the movement patterns of high-energy charged particles influenced by the Earth's magnetic field, as observed in the aurora borealis phenomenon. The section presents the mathematical foundations, pseudo-code, and a flowchart, along with an analysis of the algorithm's time complexity.

Mathematical Model of the PLO

The aurora borealis, resulting from solar-charged particles interacting with the Earth's magnetic field and atmosphere, provides the conceptual basis for the PLO. The algorithm captures the dynamic interactions between particles, magnetic fields, and atmospheric conditions, simulating behaviors such as spiraling motion, particle collisions, and eventual convergence towards the poles [34, 35].

Initialization Phase

The algorithm begins by generating an initial population of candidate solutions using a uniform pseudo-random distribution. This process is represented by:

$$(N, D) = LB + R \times (UB - LB) \quad (20)$$

The Where:

• N is the number of candidate solutions,

• D is the number of dimensions in the solution space,

• LB and UB represent the lower and upper bounds of the variables, respectively,

• R is a matrix of random values within [0, 1].

The aurora-inspired dynamics are implemented via two key mechanisms: gyration motion (local exploitation) and oval walk (global exploration). Gyration simulates local turbulence by perturbing the current solution based on nearby particle interactions. These two steps are alternated or adaptively combined during each iteration to ensure a balance between convergence (via gyration) and diversity (via oval walking).To simulate aurora-inspired motion, the PLO algorithm incorporates two main update mechanisms:

Gyration Motion (Local Exploitation)

The gyration behavior of charged particles in a magnetic field, driven by the Lorentz force, forms the foundation of this phase. The Lorentz force experienced by a particle with charge q, velocity v, and magnetic field strength B, is given by:

According to Newton's second law;

$$F_L = m\frac{dv}{dt} \quad (22)$$

Upon rearranging and integrating two sides, the following equation is derived, which explains the law governing the particle velocity in the magnetic field:

$$\frac{dv}{v} = \frac{qB}{m}dt \quad (24)$$

The velocity relationship, integrated over time and the initial velocity $_0$, is expressed as:

$$\int_{v_o}^{v} \frac{1}{v}dv = \int_0^t \frac{qB}{m}dt \quad (25)$$

The solution to this equation is given as:

Exponential conversion would be:

$$\frac{v}{v_0} = e^{qBt/m} \quad (27)$$

Upon solving and integrating, the particle velocity is presented as:

$$v\,(t) = v_0\, e^{qBt/m} \quad (28)$$

To account for atmospheric damping, a damping factor α modifies the velocity equation:

$$m\frac{dv}{dt} = qvB - \alpha v \quad (29)$$

The refined equation enhances the model's fidelity by integrating the effects of atmospheric damping, thereby improving its accuracy in simulating particle dynamics. This modification results in a nonhomogeneous first-order linear differential equation. By applying the method of variation of constants, a trial solution of the form *v*= *Ce*^{t} is assumed, where *C* and λ are constants to be determined. Substituting into the differential equation yields:

$$m\lambda Ce^{\lambda t} = qBCe^{\lambda t} - \alpha Ce^{\lambda t} \quad (30)$$

Thus, the expression for λ is obtained as $\lambda = (qB\text{-}\alpha)/m$ the general solution for the particle velocity over time becomes:

Here, *C* represents the constant of integration, and the parameters *q*, *m*, and *B* correspond to the charge carried by the particle, its mass, and the Earth magnetic field strength, respectively. For simplicity, the values of *C*, *q*, and *B* are set to 1, while *m* is assigned a value of 100. The damping factor α is treated as a random variable within the range [1,1.5]. The fitness evaluation process of the algorithm is utilized to simulate the temporal behavior (t) of Eq. (31).

$$v(t) = Ce^{\frac{(qB-\alpha)\mathrm{t}}{\mathrm{m}}} \quad (31)$$

The PLO algorithm captures a range of realistic gyration effects, including:

- Spiraling trajectories around magnetic field lines,
- Velocity attenuation due to environmental damping,
- Gradual convergence toward Polar Regions, which promotes focused local search and enhances the algorithm's exploitation capabilities.

This mechanism allows the algorithm to refine solutions near the current best candidate, mimicking the localized turbulence of auroras:

$$x_i^{(t+1)} = x_i^{(t)} + \alpha . r_1 . \left(x_{best}^{(t)} - x_i^{(t)}\right) \quad (32)$$

Where:

$x_i^{(t)}$ is the position of the *i-th* candidate solution at iteration *t*

$x_{best}^{(t)}$ is the best-known solution at iteration *t*

α is a learning rate or step-size parameter

$r_1 \in [0, 1]$ is a uniformly distributed random number

•This promotes local search around the best solution

Aurora Oval Walk (Global Exploitation)

The Aurora Oval Walk mechanism enhances the exploration capabilities of the optimization algorithm, drawing inspiration from the elliptical patterns formed by auroras under the influence of geomagnetic and atmospheric dynamics. To model this process, the Levy Flight (LF) approach—widely utilized in metaheuristics—is employed. This technique is particularly effective due to its ability to perform non-Gaussian, stochastic jumps, which aids in traversing the global solution space. The statistical formulation of LF is given by (32) and (33):

$$\text{levy}(d) \sim |d|^{-(1+\beta)},\ 0 < \beta \leq 2 \quad (33)$$

$$Ao = (d) \times (\overline{X}_j - X_{i,}) + LB + r_1 \times \frac{(UB - LB)}{2} \quad (34)$$

In this equation, X j is the center-of-mass of the population, X {i, j} represents the current particle position, LB and UB denote the lower and upper bounds of the search space, and r_1 is a random value in the interval [0, 1]. The center-of-mass, which guides global positioning, is computed as:

$$\bar{X}_j = \frac{1}{N} \sum_{i-1}^{N} X_i \quad (35)$$

This The Aurora Oval Walk mechanism strategically integrates Levy Flight to balance exploration and exploitation. While gyration motion is dedicated to refined local search, the aurora oval walk facilitates broader global search. This dual mechanism enhances the algorithm's capacity to both discover promising solution regions and finely tune solutions therein.

The integration of Levy Flight into the Polar Lights Optimization (PLO) framework is a deliberate strategy to improve global exploration efficiency. Owing to its heavy-tailed distribution, LF enables the algorithm to make substantial leaps across the solution space, thereby helping avoid premature convergence to local optima and enabling the identification of multiple optimal regions. However, the effectiveness of LF is contingent upon its statistical compatibility with the spatial complexity of the problem domain.

In the context of PEMFC (Proton Exchange Membrane Fuel Cell) parameter estimation, the search space is inherently nonlinear, featuring numerous local optima and complex interdependencies among parameters. The use of LF within the PLO algorithm effectively addresses these challenges by leveraging its capability to explore high-dimensional, rugged landscapes through sporadic long-distance moves. The combination of LF and gyration motion ensures a dynamic equilibrium between exploration and exploitation throughout the optimization process.

Empirical evaluations across six different PEMFC models validate the efficacy of LF within the PLO framework. Results indicate superior performance in terms of sum of squared errors (SSE), along with enhanced convergence speed and robustness when compared to other contemporary optimization techniques. This confirms that the statistical properties of LF are well-aligned with the structural characteristics of the PEMFC parameter estimation problem. To adaptively guide the optimization trajectory, PLO employs two weights—W_1 and W_2—which are dynamically adjusted over the course of iterations. These weights regulate the influence of the local (gyration motion) and global (LF-based aurora oval walk) search mechanisms. The composite update rule for generating a new solution is given in Eq. (35):

$$x_{new_i,} = x_i + r_2 X(W_1(t) + W_1 X(A_o)) \quad (36)$$

In this formulation, r_2 accounts for the environmental perturbations and takes a value within [0,1]. Adaptive weights w_1 and w_2, calculated using Eqs. (36) and (37), are computed as follows:

$$W_1 = \frac{2}{1 + e^{-2(t/T)^4}} - 1 \quad (37)$$

$$W_2 = e^{-(2t/T)^3} \quad (38)$$

Here, t denotes the current iteration number, and T is the maximum number of iterations. As iterations progress, W 1 increases to favor local exploitation, while W 2 decreases to prioritize global exploration in the early search phase. This dynamic weighting scheme allows the algorithm to efficiently navigate the solution space without requiring prior assumptions about the problem topology.

To mimic the elliptical motion of charged particles in auroras and ensure exploration of the global search space:

$$x_i^{(t+1)} = x_i^{(t)} + \beta . r_2 . (x_{mean}^{(t)} - x_i^{(t)}) \quad (39)$$

Where:

$x_{mean}^{(t)}$ is the mean position of all current solutions at iteration t

β is a scaling parameter controlling the exploration strength

$r_2 \sim N(0,1)$ is a normally distributed random number

This encourages diversified exploration across the solution space

In conclusion, the incorporation of Levy Flight within the PLO algorithm proves instrumental in exploring the complex, nonlinear, and high-dimensional solution space characteristic of PEMFC parameter estimation. Experimental outcomes affirm that the statistical features of LF are ideally suited to the domain's spatial requirements, leading to more robust and accurate optimization performance. Future research could explore the scalability of this approach in larger multi-component systems and assess its transferability to domains with similar spatial properties.

Particle Collision

To effectively address the challenge of local optima entrapment, the Polar Lights Optimization (PLO) algorithm incorporates a chaotic particle collision mechanism, mathematically defined as:

$$x_{new_i}, = x_i, + \, sin(r_3 \pi) \times (x_{i,j} - x_{a,j}), r_4 < K \; and \; r_5 < 0.05 \quad (40)$$

Here, the collision probability K is dynamically determined by:

$$K = \sqrt{(t/T)} \quad (41)$$

This mechanism enables dynamic modifications in both velocity and direction, significantly enhancing the algorithm's capacity for global search. Inspired by the auroral phenomena, where charged particles interact and alter their paths upon collision, the chaotic collision strategy facilitates exploration of unexplored regions within the solution space. Unlike traditional genetic algorithms (GA) and differential evolution (DE) methods that apply uniform crossover and mutation operations across the population—often leading to premature convergence and limited diversity—the targeted collision approach in PLO induces controlled stochasticity. This enables landscape-sensitive perturbations, making it an effective strategy for escaping local optima.

The Proposed PLO Algorithm

The Polar Lights Optimization (PLO) algorithm draws inspiration from the motion of charged particles within Earth's magnetosphere, particularly the formation of auroral ovals due to Lorentz force dynamics and atmospheric influences.

These particles follow elliptical trajectories converging near the magnetic poles. The PLO algorithm models this behavior through a combination of gyration motion for local exploitation and auroral oval walk for global exploration. Damping factors are incorporated to improve the fidelity of the physical modeling.

While this study focuses on minimizing single-objective sum of squared errors (SSE), the PLO algorithm demonstrates potential in solving multi-objective problems by using weighted aggregations of performance metrics in its fitness function. The fitness function not only determines convergence speed and stability but also establishes a smooth, continuous search landscape conducive to efficient exploration.

Through the gyration motion, the algorithm ensures fine-tuned local search, facilitating rapid convergence to optimal solutions. Simultaneously, the auroral oval walk supports broader exploration to avoid entrapment in local minima. The chaotic particle collision mechanism introduced in Equation (38) acts as a perturbation strategy that sustains population diversity and enhances both convergence rate and solution quality. Experimental results confirm that PLO consistently achieves rapid convergence—within the initial 50 iterations—across all tested scenarios, outperforming methods such as GSA and DE which demonstrate slower stabilization.

To provide structural transparency, the algorithm is presented through a detailed pseudo-code (Algorithm 1) and visually through a flowchart (Figure 3) that outlines each operational step.

To address potential concerns related to computational efficiency, the time complexity of the PLO algorithm has been comprehensively analyzed. The preliminary assessment identified key contributors to complexity Gyration motion: $((n\ X\ d))$, auroral oval walk $((n\ X\ d))$, and Fitness evaluations: $((n\ X\ log_n))$,

A more detailed formulation takes into account additional components such as adaptive weight updates, chaotic particle collisions, and the dynamic nature of the search process. The total time complexity is thus represented as Total Complexity = $0(n\ x\ d\ x\ t) + 0(n\ x\ d\ x\ k) + (n\ x\ log_n)$, here $0(0(n\ x\ d\ x\ t)$) accounts for both the gyration motion and aurora oval walk, $0(n\ x\ d\ x\ k)$ represents the cost associated with the particle collision mechanism., and 0 $(n\ x\ d\ x\ k)$ reflects the cost of fitness evaluations.

Although adaptive weights involve exponential calculations, they are updated once per iteration, maintaining a linear complexity with respect to population size n. The dynamic interactions between gyration and aurora-based motion ensure that the computational overhead remains manageable, particularly since the probabilistic nature of the collision mechanism introduces only a logarithmic dependence on the number of iterations.

This balance ensures that diversity is preserved without significantly affecting performance, making PLO suitable for large-scale, high-dimensional optimization tasks.

The overall complexity includes contributions from gyration motion $((n\ x\ d))$, auroral oval walk $((n\ x\ d))$, and fitness evaluations $((n\ x\ log_n))$, resulting in Total Complexity = $(n\ x\ d)+(n\ x\ d)+(n\ x\ log_n)$.

Algorithm 1 PLO's pseudo-code

Parameters initializing: $FEs = 0$, $MaxFEs$, $t = 0$
Initialize high-energy particle cluster X.
Calculate the fitness value $f(X)$.
Sort X according to $f(X)$.
Update the current optimal solution X_{best}.
While $FEs < MaxFEs$
  Calculate the velocity $v(t)$ for each particle, according to Eq. (31).
  Calculate aurora oval walk Ao for each particle, according to Eq. (33).
  Calculate weights W_1 and W_2 according to Eq. (36) and Eq. (37).
  For each energetic particle **do**
    Updating particles X_{new} using Eq. (35).
    If $r_4 < K$ and $r_5 < 0.05$
      Particle collision strategy: update particle X_{new} using Eq. (38).
    End If
      Calculate the fitness $f(X_{new})$.
      $FEs = FEs + 1$.
  End For
    If $f(X_{new}) < f(X)$
      Iterating over X using the greedy selection mechanism.
    End If
  Sort X according to $f(X)$.
  Update the optimal solution X_{best}.
  $t = t + 1$.
End While
Return the X_{best}.

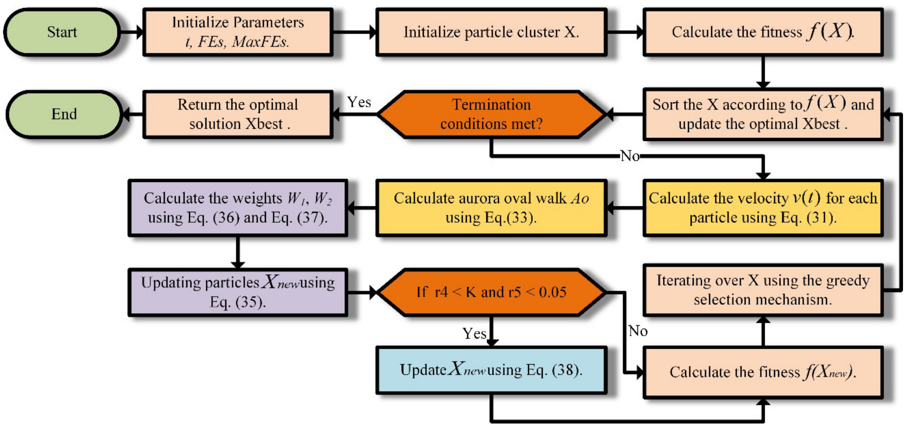

Figure 4: The flowchart of PLO

Result Analysis and Discussion

Result Analysis

The proposed Polar Lights Optimization (PLO) algorithm was rigorously evaluated against nine contemporary optimization algorithms—Gravitational Search Algorithm (GSA), Differential Evolution (DE), Particle Swarm Optimization (PSO), Moth Flame Optimization (MFO), Ant Colony Optimization for Continuous Domains (ACOR), Multi-Verse Optimizer (MVO), Whale Optimization Algorithm (WOA), Sine Cosine Algorithm (SCA), and JAYA. The evaluation was conducted using six Proton Exchange Membrane Fuel Cell (PEMFC) models: BCS 500 W, Nedstack 600 W PS6, SR-12 W, Horizon H-12, Ballard Mark V, and STD 250 W Stack. Polarization curve data used for these models were extracted from prior research [Ref. 58]. The BCS 500 W model served as the baseline for comparison, while the Nedstack 600 W PS6 consisted of 65 cells (each with a surface area of 240 cm^2 and thickness of 178 mm), and the Horizon H-12 was composed of 36 series-connected cells supporting a maximum current output of 30 A.

All simulations were executed in MATLAB R2016b on a computing platform equipped with an Intel Core i7 processor and 16 GB RAM. Comparative results indicate that the PLO algorithm consistently outperformed all other algorithms in terms of minimizing the Sum of Squared Errors (SSE), demonstrating superior convergence behavior, predictive accuracy, and robustness in modeling PEMFC dynamics. To ensure statistical validity, each algorithm underwent 30 independent runs on each of the six models. A key aspect of the PLO algorithm's performance is its sensitivity to control parameters. Unlike conventional algorithms that require manual parameter tuning, PLO employs an adaptive strategy where parameters such as W1 and W2 are derived from auroral dynamics and updated dynamically to strike a balance between exploration and exploitation. The adaptive weight mechanism is governed by Equations (36) and (37), where:

$W_1 = 2/(1 + e^{-2(t/T)^4}) - 1$ and $W = e^{-2(t/T)^3}$ These expressions ensure that W_1 increases over time to favor local exploitation during later iterations, while W_2 decreases, enhancing global exploration in the early stages of the optimization. This adaptive weighting framework allows PLO to self-tune based on the complexity and dimensionality of the optimization problem, thus enhancing its generalizability and applicability. Moreover, the damping factor \alpha, which influences the velocity update during gyration motion, is randomly selected within the interval [1, 1.5], introducing beneficial stochastic variability into the search process. The inclusion of Levy Flight within the aurora oval walk further augments this adaptability by enabling non--Gaussian jumps, particularly effective for complex, high-dimensional optimization landscapes. This integration of stochastic elements and adaptive parameterization minimizes the sensitivity of the algorithm to initial settings, thereby improving reliability across diverse scenarios.

The algorithm employs several stopping criteria to ensure computational efficiency. One primary criterion is the maximum iteration limit T = 500, which halts the algorithm after a fixed number of iterations suitable for large-scale optimization tasks. Another is the fitness threshold, which terminates the search once the SSE reaches an acceptable value, avoiding unnecessary computation.

Additionally, a stagnation detection mechanism ends the process if no significant improvements in fitness are observed over a set number of iterations, preventing wasteful computation when convergence has effectively been achieved.

Key control parameters are defined alongside the stopping criteria to regulate search behavior. The population size N = 40 determines the number of candidate solutions; while larger populations enhance diversity and exploration capacity, they also increase computational load. Conversely, smaller populations may lead to premature convergence due to insufficient diversity. The dimensionality D of the problem is set based on the number of parameters in the PEMFC model, which includes seven critical variables: ξ_1, ξ_2, ξ_3, ξ_4, λ, R_C, and b.

Appropriate upper and lower bounds (UB, LB) are established for each parameter to ensure that the solutions remain physically feasible. These bounds guide the search process within realistic regions of the solution space, avoiding unphysical or non-viable results. The damping factor \alpha, with a range between 1 and 1.5, simulates atmospheric damping experienced by charged particles and plays a crucial role in the velocity update process during gyration. By dynamically adjusting search intensity, it contributes to avoiding local minima and maintaining effective performance without excessive computational cost.

Table 1: Default parameter settings of the compared algorithms

Algorithms and their Default settings
Gravitational Search Algorithm (GSA) [53] -R_{norm} = 2
DE [54] – F [0.4,0.9]& CR [0.1,0.9]
Particle Swarm Optimizer (PSO) [55] – c_1= 2; c_2= 2; V_{max}= 6
Moth-Flame Optimization Algorithm (MFO) [56]- k = 10; q= 0.5; *ibslo*= 1
Ant Colony Optimization for Continuous Domains (ACOR) [57] - k = 10; q = 0.5; *ibslo* = 1
Multi-Verse Optimizer (MVO) [58]-W_{max}= 1; W_{min}= 0.2
Whale Optimization Algorithm (WOA) [59]- α_1 = [2,0]; α_2= [−2, −1]; b= 1
Sine Cosine Algorithm (SCA) [60]- α = 2
Jaya Optimization Algorithm (JAYA) [61] - *(no specific parameters provided)*
Polar Lights Optimization (PLO) [47]-m = 100; a= [1,1.5]

Table 2: PEMFC Operating Condition use for analysis

S. No.	PEMFC Type	Power(W)	Ncells (no)	A(cm^2)	I(um)	T(K)	Jmax(mA/cm^2)	PH2(bar)	PO2(bar)
1	BCS 500 W	500	32	64	178	333	469	1.0	0.2095
2	NetStack PS6	6000	65	240	178	343	1125	1.0	1.0
3	SR-12	500	48	62.5	25	323	672	1.47628	0.2095
4	Horizon H-12	12	13	8.1	25	328.15	246.9	0.4935	1.0
5	Ballard Mark V	5000	35	232	178	343	1500	1.0	1.0
6	STD 250 W	250	24	27	127	343	860	1.0	1.0

Result Analysis for Polar Lights Optimization (PLO) on BCS 500 W PEMFC

The application of the Polar Lights Optimization (PLO) algorithm to the BCS 500 W PEMFC model demonstrates its high accuracy and robustness in parameter estimation. The algorithm's performance is substantiated by quantitative results presented in Table 3 and visual analyses in Figure 4. The optimized parameters ξ_1, ξ_2, ξ_3, ξ_4, λ, R_C and B—exhibit strong alignment with the expected physical characteristics of PEMFCs. For example, PLO estimates the membrane resistance as Rc = 0.0001, consistent with the low-resistance requirements necessary for effective fuel cell performance. Similarly, the estimated polarization coefficients (ξ_1=−0.8532, ξ_2= 0.00218, ξ_3= 0.000036, ξ_4= −0.00019) accurately reflect the complex nonlinear electrochemical dynamics intrinsic to PEMFC systems, thereby affirming the algorithm's ability to capture system behavior with precision.

Statistical performance metrics further support PLO's superiority. The algorithm achieved the lowest mean fitness value (Mean = 0.025519) across all tested approaches, accompanied by an exceptionally low standard deviation (*std*= 5.92×10^{-5}), signifying not only accuracy but also consistency in repeated runs. Additionally, PLO demonstrated the best computational efficiency, achieving a runtime of only 0.176648 seconds, and secured the top position in the Friedman Ranking (FR = 1.2), highlighting its speed and stability compared to other state-of-the-art algorithms. Figure 4(a) presents the voltage-current (V-I) and power--voltage (P-V) curves along with the absolute error (AE) and relative error (RE%) plots. The close overlap between the simulated and measured V-I and P-V curves signifies the high fidelity of PLO's parameter estimation. The error analysis reveals low error margins across all current levels, with peak deviations remaining well within acceptable boundaries, confirming the reliability of the algorithm. In Figure 4(b), the convergence curves demonstrate that PLO rapidly reaches an optimal solution within the first 100 iterations—significantly outperforming algorithms like GSA and DE, which show delayed convergence and greater fluctuation.

Figure 4(c) provides a comparative boxplot of fitness values across algorithms. PLO displays a tightly clustered distribution with minimal variance and absence of outliers, reinforcing its robustness and consistent behavior. In contrast, algorithms such as GSA and JAYA reveal wider distributions and multiple outliers, indicating greater variability and less reliable convergence performance.

In conclusion, the analysis clearly indicates that PLO excels in estimating the parameters of the BCS 500 W PEMFC. It exhibits convergence behavior typical of efficient stochastic algorithms—rapid convergence, low variance, and robust solution quality over multiple trials. These outcomes underscore the potential of PLO for broader application in large-scale or more complex fuel cell systems. Future studies may focus on scaling the algorithm for high-dimensional models and evaluating its adaptability under diverse operational environments.

Table 3: Optimized parameters, SSE values, runtime, and rankings for BCS 500W using PLO and other algorithms

Algorithm	GSA	DE	PSO	MFO	ACOR	MVO	WOA	SCA	JAYA	PLO
ξ_1	-0.98401	-1.17707	-0.8532	-0.87108	-1.15643	-0.95535	-1.12095	-1.1723	-0.96462	-0.8532
ξ_2	0.00301	0.003251	0.003079	0.002331	0.00337	0.002577	0.003231	0.003733	0.002851	0.00218
ξ_3	6.45E-05	4.23E-05	9.39E-05	4.23E-05	5.4E-05	4.18E-05	5.19E-05	7.43E-05	5.85E-05	0.000036
ξ_4	-0.00018	-0.00019	-0.00019	-0.00019	-0.00019	-0.00019	-0.00019	-0.00019	-0.00018	-0.00019
λ	20.68135	20.16795	23	21.58818	20.88868	21.55567	20.94073	20.88438	16.61556	20.87724
R_C	0.000751	0.00012	0.000282	0.000217	0.000105	0.000157	0.000106	0.0001	0.000323	0.0001
B	0.0136	0.015599	0.016265	0.015927	0.016108	0.015973	0.016076	0.016131	0.013744	0.016126
Min. SSE	0.055008	0.026139	0.025656	0.025942	0.025505	0.02618	0.025546	0.025493	0.073793	0.025493
Max. SSE	0.19249	0.031945	0.085535	0.033361	0.025796	0.049968	0.026142	0.025646	0.140884	0.025625
Mean SSE	0.113376	0.028178	0.046848	0.029216	0.025631	0.033557	0.025789	0.025532	0.098178	0.025519
SD SSE	0.053443	0.002446	0.022626	0.003695	0.000119	0.009998	0.000233	6.39E-05	0.028865	5.92E-05
RT	3.545595	4.369544	3.249597	3.110436	6.040271	3.738654	3.658803	4.063369	6.347523	0.176648
FR	9.4	5.8	7.6	6.2	3.2	6.6	3.8	2	9.2	1.2

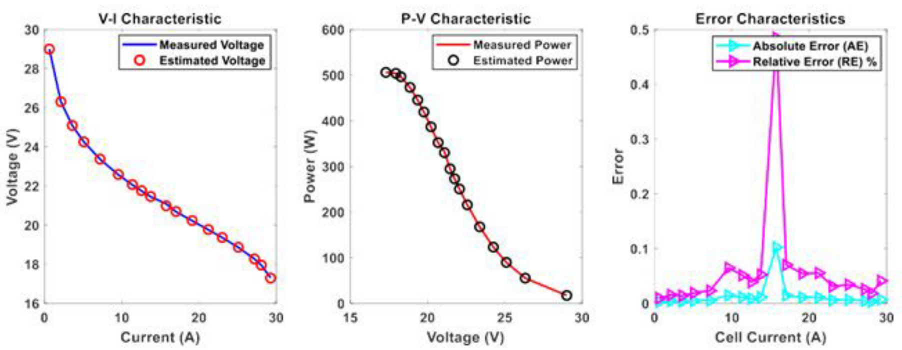

(a)

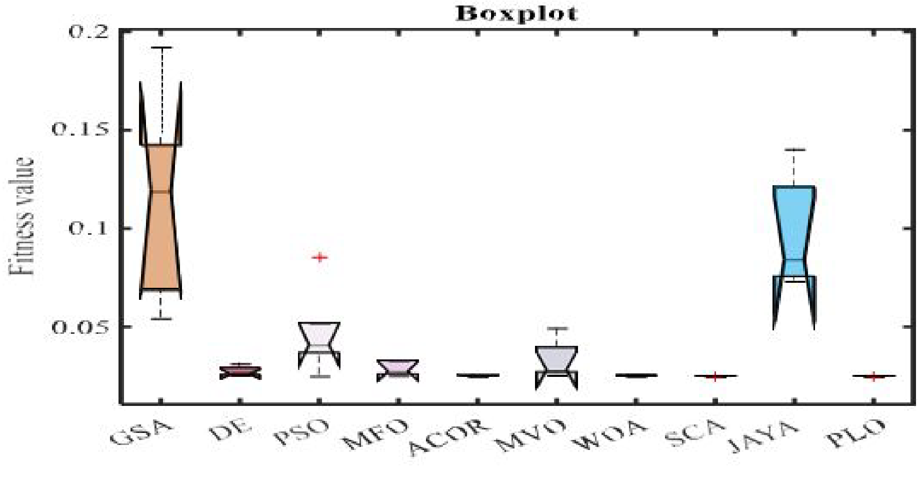

(b)

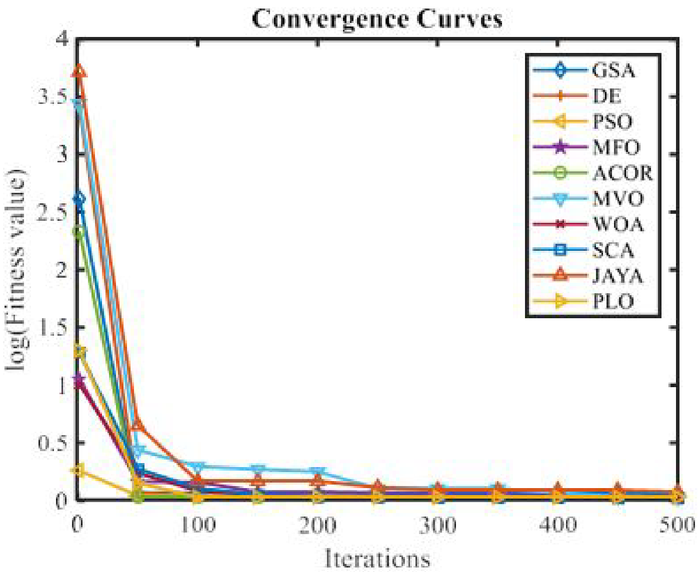

(c)

Figure 4: BCS 500W (a) V-I, P-V, and error characteristics for the BCS 500 W PEMFC using PLO. (b) Convergence curve of PLO, (c) Boxplot of fitness values for PLO to other algorithms

Polar Lights Optimization Result Analysis (PLO) on Nedstack 600 W PS6 PEMFC

The application of the Polar Lights Optimization (PLO) algorithm to the Nedstack 600 W PS6 PEMFC model further confirms its effectiveness in capturing complex nonlinear system behaviors and minimizing the Sum of Squared Errors (SSE). As evidenced through tabulated results and visual figures, PLO delivers superior performance across multiple dimensions. Table 4 provides a comprehensive summary of the optimized parameters and comparative statistical metrics for PLO and alternative algorithms. Notably, PLO achieved the lowest SSE values, recording a minimum and mean SSE of 0.275211 with an exceptionally low standard deviation of (5.84×10^{-16}). This negligible variance indicates remarkable repeatability and robustness across independent optimization runs.

In terms of computational efficiency, PLO also demonstrated significant advantages. Its execution time (RT = 0.200966 s) was markedly faster than that of competing methods such as DE (5.120299 s) and JAYA (9.062881 s), reflecting its ability to achieve optimal solutions with minimal computational overhead. Furthermore, PLO secured the top position in the Friedman Ranking (FR = 1), reinforcing its superiority in both accuracy and efficiency within this benchmark scenario.

Visual analyses further validate the algorithm's effectiveness. Figure 5(a) presents the voltage-current (V-I) and power-voltage (P-V) curves, along with the error profiles. The V-I and P-V plots reveal strong congruence between the estimated and experimental data, highlighting PLO's precision in replicating system behavior. The associated error plots confirm low absolute error (AE) and relative error percentage (RE%) across the current range, including higher current densities, ensuring reliable prediction throughout the operational spectrum.

Figure 5(b) illustrates the convergence patterns of PLO against other algorithms. PLO attains rapid convergence within the first 50 iterations—substantially faster than most competitors—demonstrating its capacity for swift and stable solution identification. The fitness value boxplot in Figure 5(c) depicts the distribution of performance across multiple runs. PLO displays the narrowest interquartile range and the lowest median fitness value, underscoring its consistency and reliability. In contrast, GSA and JAYA exhibit broader distributions and higher variability, suggesting less stable performance across trials.

Overall, the findings affirm the exceptional capability of PLO in parameter optimization for the Nedstack 600 W PS6 PEMFC. The algorithm achieves highly accurate, consistent, and computationally efficient results, making it a promising tool for precision modeling of PEMFC systems. These outcomes also support the algorithm's potential scalability and applicability in broader and more complex energy systems. Future investigations may extend its validation under dynamic load conditions and real-time implementation scenarios to further substantiate its robustness and adaptability.

Table 4: Optimized parameters, SSE values, runtime, and rankings for Nedstack 600W PS6 using PLO and other algorithms

Algorithm	GSA	DE	PSO	MFO	ACOR	MVO	WOA	SCA	JAYA	PLO
ξ_1	-1.10315	-0.8532	-1.15235	-0.96635	-0.87151	-0.8532	-0.88116	-1.08097	-0.8968	-0.85498
ξ_2	0.003835	0.002397	0.00327	0.002858	0.002482	0.002532	0.003005	0.003235	0.002763	0.002438
ξ_3	8.64E-05	0.000036	0.000036	4.54E-05	3.82E-05	4.55E-05	7.35E-05	4.84E-05	5.21E-05	3.85E-05
ξ_4	-9.5E-05	-9.5E-05	-9.5E-05	-9.5E-05	-9.5E-05	-9.5E-05	-9.5E-05	-9.5E-05	-9.5E-05	-9.5E-05
λ	15.53654	14	14	14	14.00135	14	14	14.00281	21.81007	14
R_C	0.0001	0.000103	0.00012	0.000106	0.00012	0.000121	0.000123	0.000108	0.000399	0.00012
B	0.03593	0.019297	0.016788	0.018753	0.01698	0.016909	0.016248	0.018615	0.026352	0.016788
Min. SSE	0.29739	0.275746	0.275211	0.275581	0.275228	0.275346	0.275305	0.275762	0.334858	0.275211
Max. SSE	0.837166	0.319379	0.320685	0.295621	0.286627	0.300545	0.276626	0.285955	0.467356	0.275211
Mean SSE	0.494496	0.292274	0.284815	0.281789	0.281106	0.281489	0.275946	0.278785	0.416984	0.275211
SD SSE	0.215484	0.017628	0.020055	0.008152	0.004777	0.010691	0.000477	0.004319	0.05035	5.84E-16
RT	4.510984	5.120299	4.323254	4.446581	8.84278	4.906147	4.900548	5.558625	9.062881	0.200966
FR	9.6	6.8	4	5.2	5.2	5.4	3.8	4.6	9.4	1

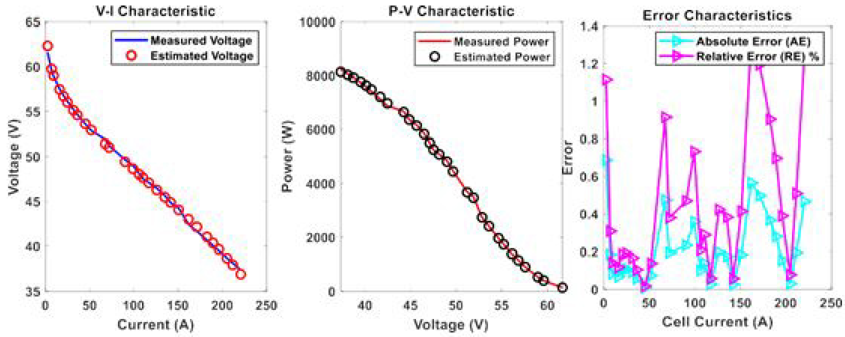

(a)

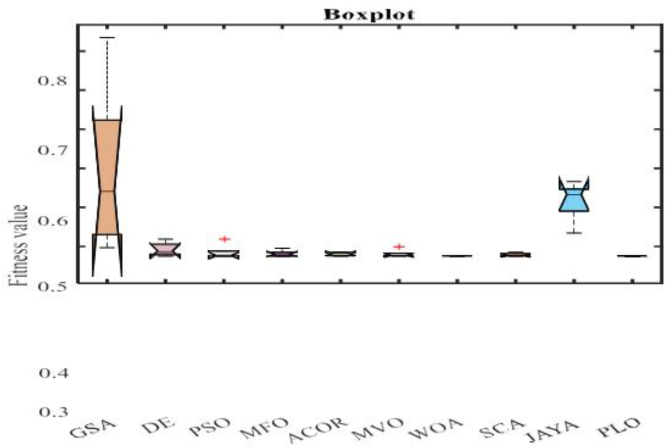

(b)

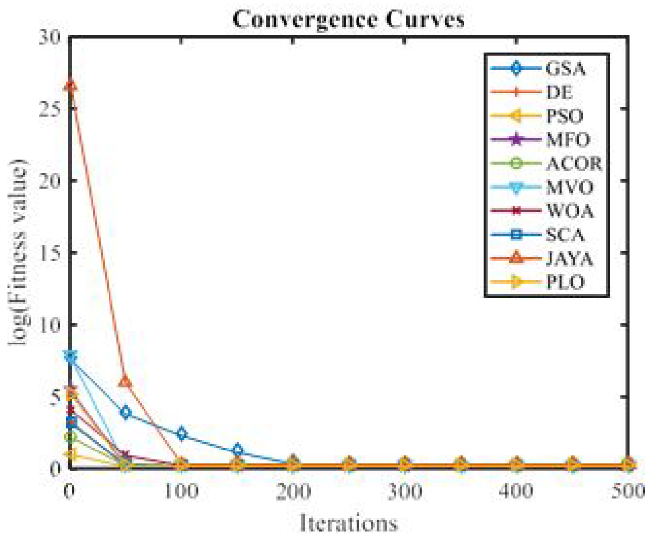

(c)

Figure 5: Nedstack 600W PS (a) V-I, P-V, and error characteristics for the BCS 500 W PEMFC using PLO. (b) Convergence curve of PLO, (c) Boxplot of fitness values for PLO to other algorithms.

Result Analysis for PLO on SR-12 W PEMFC

The PLO algorithm has proven to be highly effective in optimizing the SR-12 W PEMFC, achieving outstanding results in reducing the sum of squared errors (SSE) and accurately capturing the system's essential characteristics. The performance outcomes are thoroughly detailed through tables and clear figure descriptions. Table 5 presents a statistical comparison of SSE values for the PLO and other competing algorithms. Notably, PLO achieves the lowest minimum SSE (0.242284) and mean SSE (0.242413), along with a very small standard deviation of SSE (0.000288). This reflects the algorithm's strong consistency and precision across various trials. Additionally, its runtime (RT = 0.114637 s) indicates remarkable computational efficiency when compared to other methods such as JAYA (RT = 6.468212 s) and GSA (RT = 3.169781 s). The high fitness ratio (FR = 2.2) further underscores its superior performance in this analysis.

Figure 6(a): The voltage-current (V-I) and power-voltage (P-V) curves reveal an excellent correlation between measured and predicted values, while the error characteristics show minimal deviations, maintaining low absolute error (AE) and relative error percentages (RE%) across the current spectrum. Figure 6(b): The PLO algorithm demonstrates rapid convergence, stabilizing within the first 50 iterations, significantly outperforming algorithms with slower convergence rates such as GSA and MVO. Figure 6(c): The boxplot illustrates the reliability of PLO, with fitness values tightly grouped and minimal variance, contrasting with the broader distributions observed in algorithms like GSA and JAYA.

Table 5: Optimized parameters, SSE values, runtime, and rankings for SR-12 W using PLO and other algorithms

Algorithm	GSA	DE	PSO	MFO	ACOR	MVO	WOA	SCA	JAYA	PLO
ξ_1	-1.19268	-0.86141	-0.8532	-1.03159	-0.88797	-0.9303	-1.02158	-0.94242	-0.91562	-0.89596
ξ_2	0.003894	0.003273	0.003251	0.003157	0.003026	0.002725	0.003539	0.00283	0.002571	0.002421
ξ_3	7.19E-05	9.78E-05	0.000098	5.65E-05	7.67E-05	4.86E-05	8.31E-05	5.31E-05	4.13E-05	0.000036
ξ_4	-9.5E-05	-9.5E-05	-9.5E-05	-9.5E-05	-9.5E-05	-9.5E-05	-9.5E-05	-9.5E-05	-9.6E-05	-9.5E-05
λ	23	22.69424	23	19.66628	22.97157	14.84181	22.79868	22.81813	18.93848	23
RC	0.0001	0.000783	0.0008	0.000603	0.000671	0.000733	0.000646	0.000666	0.000541	0.000673
B	0.189474	0.173043	0.172796	0.175583	0.17533	0.170209	0.175742	0.175405	0.177995	0.17532
Min. SSE	0.260359	0.242641	0.242716	0.242443	0.242286	0.243937	0.242365	0.242293	0.25835	0.242284
Max. SSE	0.666933	0.245315	0.246387	0.245921	0.242614	0.248789	0.242628	0.242529	0.57641	0.242927
Mean SSE	0.395458	0.243985	0.244869	0.243497	0.242418	0.245324	0.242493	0.242421	0.438272	0.242413
SD SSE	0.171831	0.001088	0.00133	0.001408	0.000136	0.001984	0.000111	8.47E-05	0.15043	0.000288
RT	3.169781	3.331272	2.871496	2.971452	6.162372	3.450236	3.607356	4.233008	6.468212	0.114637
FR	9.4	5.8	7	5.4	2.6	7.2	3.2	2.6	9.6	2.2

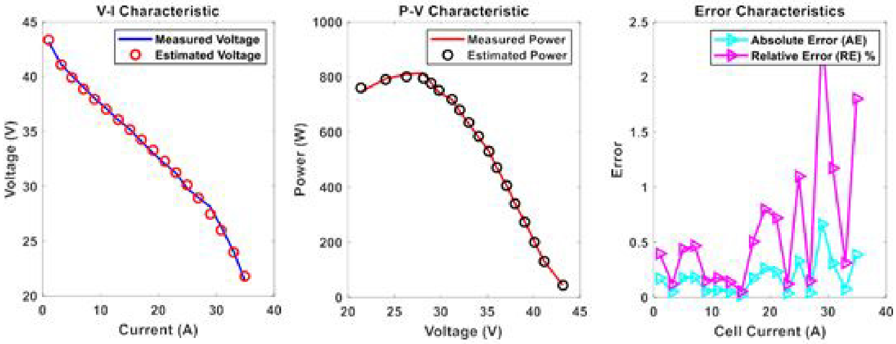

(a)

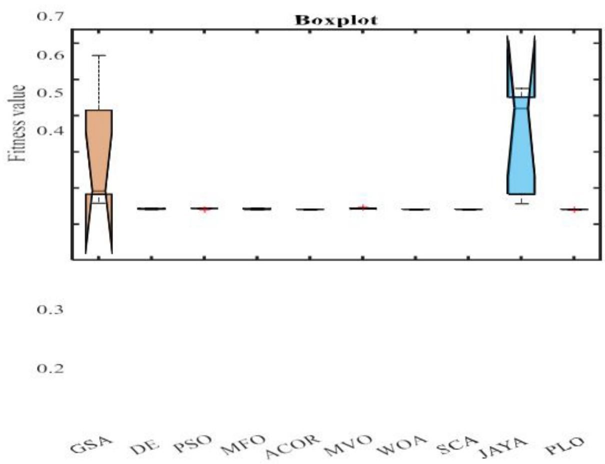

(b)

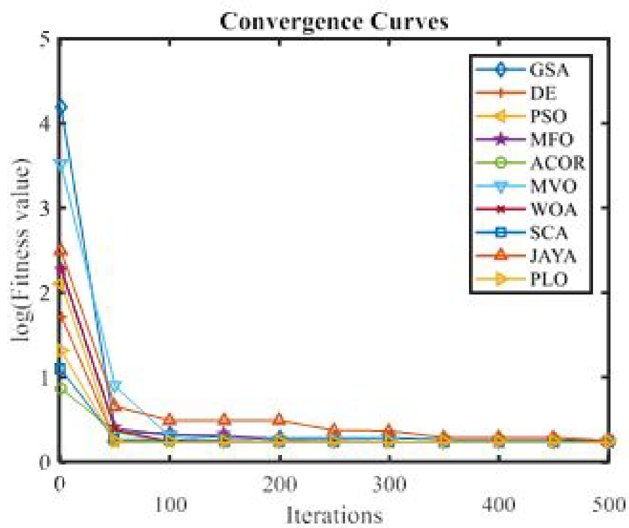

(c)

Figure 6: SR 12-W (a) V-I, P-V, and error characteristics for the BCS 500 W PEMFC using PLO. (b) Convergence curve of PLO, (c) Boxplot of fitness values for PLO to other algorithms

Result Analysis for PLO on Horizon H-12 PEMFC

PLO exhibits outstanding performance in the modeling and optimization of the Horizon H-12 PEMFC, achieving remarkable results in minimizing the sum of squared errors (SSE), enhancing computational efficiency, and maintaining consistency across iterations. The accompanying tables and succinct figures offer valuable insights into its effectiveness. Table 6 illustrates the performance of PLO in reducing SSE, where it achieves both the lowest minimum SSE (0.102915) and mean SSE (0.102915), with an almost negligible standard deviation of SSE (3.8 × 10−17), highlighting its accuracy and reliability across multiple trials. The runtime (RT = 0.127769 s) is significantly shorter than that of other algorithms, such as JAYA (RT = 6.420775 s) and GSA (RT = 3.222671 s), further affirming its computational efficiency. Additionally, PLO ranks highest with a Friedman Ranking (FR = 1).

Figure 7(a): The voltage-current (V-I) and power-voltage (P-V) curves demonstrate a close correspondence between measured and predicted values, while the error characteristics graph indicates consistently low absolute error (AE) and relative error percentages (RE%) throughout the current range. Figure 7(b): The convergence curve illustrates rapid stabilization within the initial 50 iterations, highlighting PLO's efficiency in attaining optimal solutions compared to other algorithms. Figure 7(c): The boxplot displays tightly grouped fitness values for PLO with minimal variance, contrasting sharply with the wider distributions observed in algorithms such as JAYA and GSA.

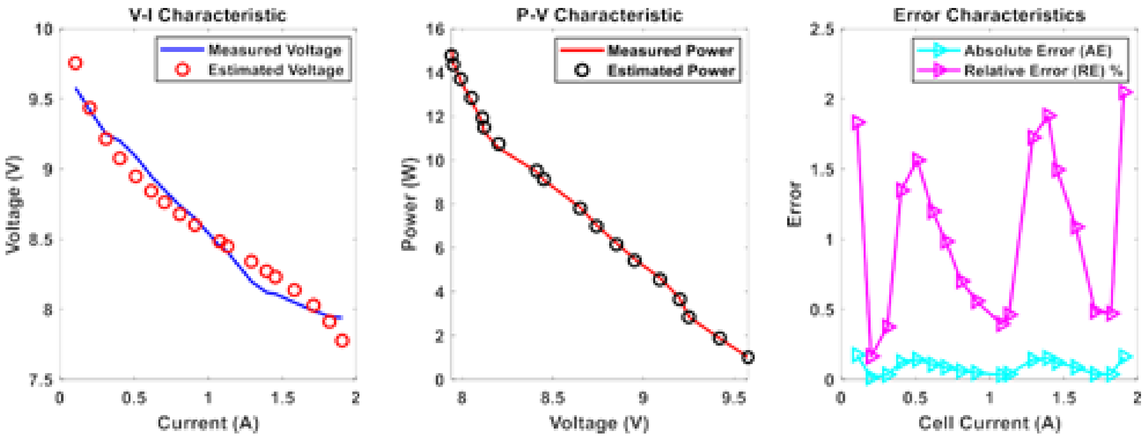

(a)

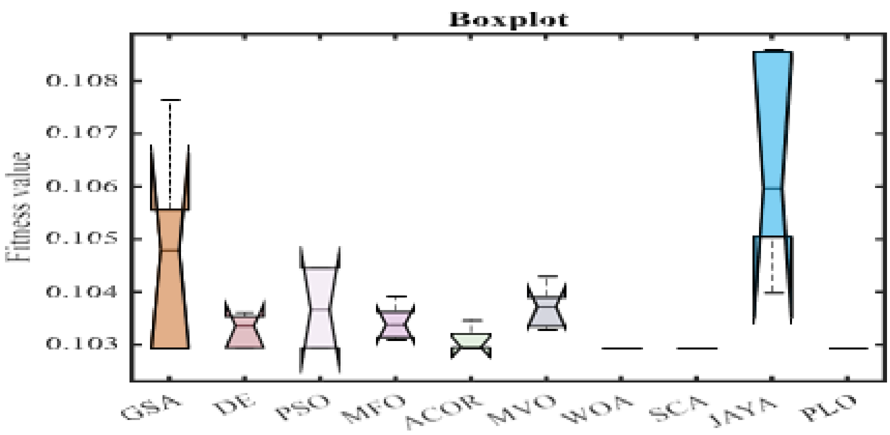

(b)

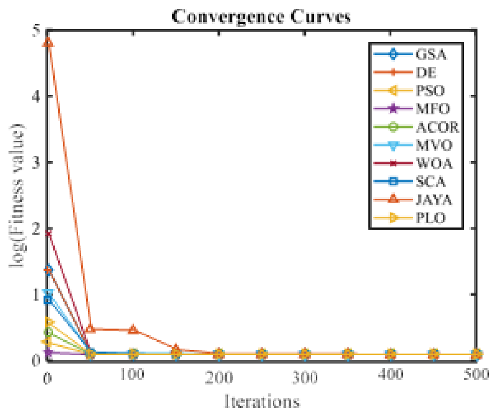

(c)

Figure 7: H-12 (a) V-I, P-V, and error characteristics for the BCS 500 W PEMFC using PLO. (b) Convergence curve of PLO, (c) Boxplot of fitness values for PLO to other algorithms.

Table 6: Optimized parameters, SSE values, runtime, and rankings for Horizon H-12 using PLO and other algorithms

Algorithm	GSA	DE	PSO	MFO	ACOR	MVO	WOA	SCA	JAYA	PLO
ξ_1	-1.1991	-0.85741	-1.19969	-0.99876	-0.98961	-0.87395	-0.86989	-1.10522	-1.19969	-1.0506
ξ_2	0.002579	0.00188	0.003445	0.002693	0.002003	0.002408	0.002133	0.00302	0.002736	0.002454
ξ_3	0.000036	6.17E-05	0.000098	8.87E-05	4.12E-05	0.000096	7.72E-05	8.85E-05	4.72E-05	0.00006
ξ_4	-0.00011	-0.00011	-0.00011	-0.00011	-0.00011	-0.00011	-0.00011	-0.00011	-0.00012	-0.00011
λ	14	14	14	14.05763	14	14	14	14.00338	14.61221	14
RC	0.0008	0.0008	0.0008	0.000661	0.0008	0.000509	0.0008	0.0008	0.000798	0.0008
B	0.0136	0.0136	0.0136	0.013616	0.0136	0.013865	0.0136	0.013601	0.013759	0.0136
Min. SSE	0.102915	0.102915	0.102915	0.103076	0.102915	0.103278	0.102915	0.102916	0.103973	0.102915
Max. SSE	0.107645	0.103578	0.104428	0.103905	0.10345	0.104292	0.102915	0.102919	0.108593	0.102915
Mean SSE	0.104622	0.103245	0.103665	0.103397	0.103069	0.103677	0.102915	0.102918	0.106491	0.102915
SD SSE	0.001938	0.000314	0.000757	0.000334	0.00023	0.000402	2.72E-07	0.000001	0.002025	3.8E-17
RT	3.222671	3.308974	2.922192	3.015107	6.14788	3.485832	3.544352	4.104557	6.420775	0.127769
FR	7.4	5	5.6	7	5.2	7	2.8	4.2	9.8	1

Result Analysis for PLO on Ballard Mark V PEMC

PLO exhibits outstanding performance in optimizing the Ballard Mark V PEMFC, achieving the lowest minimum SSE (0.148632), mean SSE (0.148632), and an almost negligible standard deviation of SSE ($4.2 \times 10-16$). These results indicate exceptional accuracy and stability, as detailed in Table 7. Additionally, the algorithm records the fastest runtime (RT = 0.107168 s) among all evaluated methods, along with a top Friedman Ranking (FR = 1), highlighting its computational efficiency.

Figure 8(a) illustrates a strong correlation between the measured and predicted voltage-current (V-I) and power-voltage (P-V) characteristics, with minimal error deviations. Figure 8(b) indicates that PLO achieves rapid convergence within the first 50 iterations, while Figure 8(c) showcases tightly clustered fitness values, reflecting its consistency in performance compared to the wider variances observed in other algorithms.

Table 7: Optimized parameters, SSE values, runtime, and rankings for Ballard Mark V using PLO and other algorithms

Algorithm	GSA	DE	PSO	MFO	ACOR	MVO	WOA	SCA	JAYA	PLO
ξ_1	-1.04515	-1.03065	-1.19969	-0.87553	-0.90709	-0.87803	-1.09292	-1.09967	-0.87362	-0.93829
ξ_2	0.003144	0.003174	0.004138	0.002598	0.002705	0.002581	0.003587	0.003165	0.002645	0.003169
ξ_3	5.96E-05	6.43E-05	0.000098	5.55E-05	5.66E-05	5.38E-05	8.09E-05	4.94E-05	6.01E-05	8.32E-05
ξ_4	-0.00017	-0.00018	-0.00017	-0.00017	-0.00017	-0.00017	-0.00017	-0.00017	-0.00016	-0.00017
λ	14.16512	16.28909	14.43912	14.63427	14.55899	14.68897	14.67389	14.462	14	14.43913
RC	0.00011	0.000289	0.0001	0.000154	0.000144	0.000124	0.000125	0.0001	0.000575	0.0001
B	0.0136	0.016091	0.013795	0.013997	0.013816	0.014246	0.014071	0.01383	0.0136	0.013795
Min. SSE	0.149733	0.150516	0.148632	0.148744	0.148718	0.148733	0.148727	0.148633	0.168511	0.148632
Max. SSE	0.155617	0.155266	0.149959	0.151388	0.149417	0.151125	0.148811	0.148692	0.232626	0.148632
Mean SSE	0.152059	0.152596	0.149069	0.149644	0.149067	0.150006	0.14876	0.148646	0.196065	0.148632
SD SSE	0.003012	0.001963	0.000602	0.001029	0.000293	0.000883	3.98E-05	2.56E-05	0.025611	4.2E-16
RT	2.857204	2.988658	2.499256	2.658668	5.500611	3.112195	3.137738	3.85156	5.57592	0.107168
FR	8	8.6	3.6	6	4.8	6.8	3.8	2.4	10	1

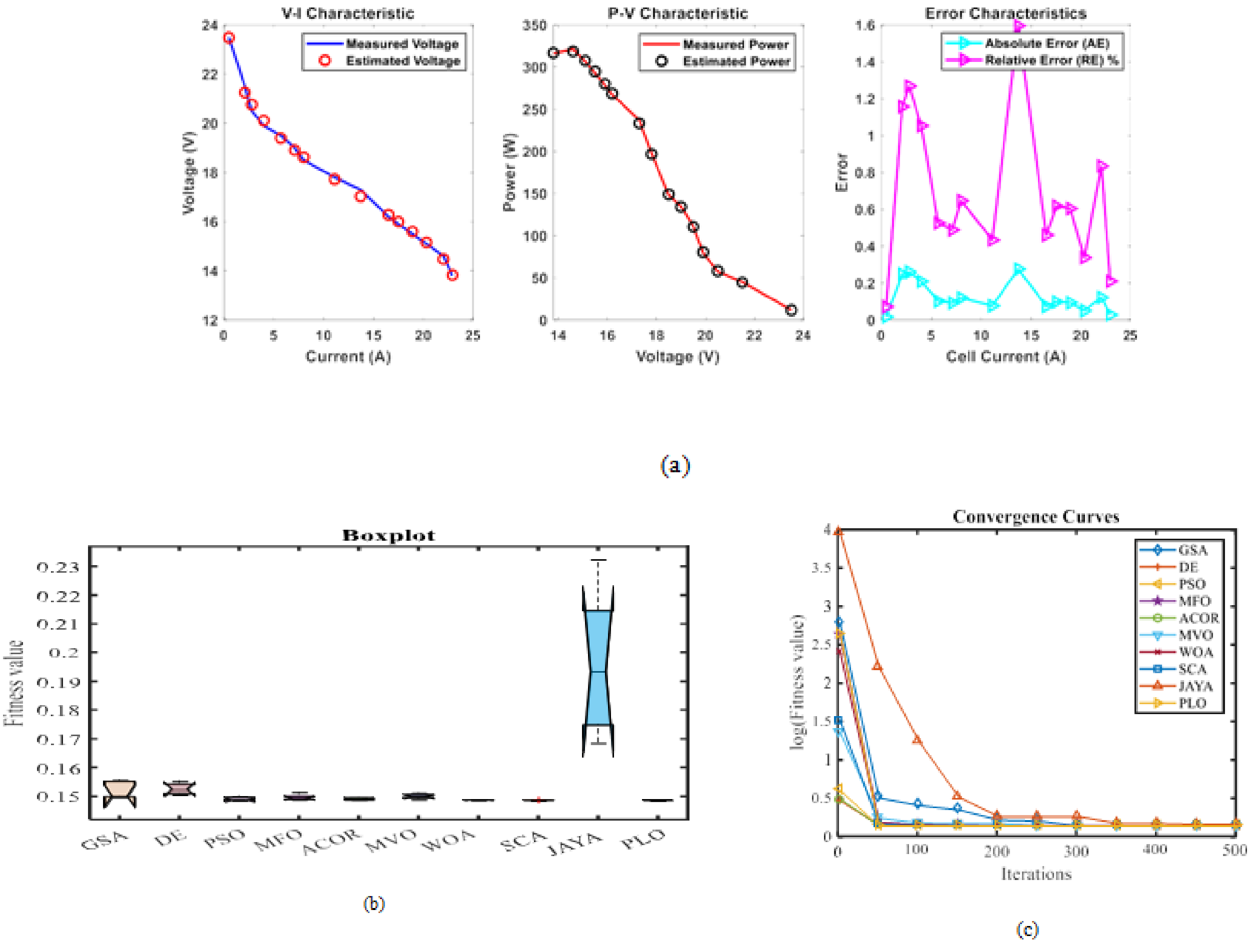

Figure 8: Ballard Mark V (a) V-I, P-V, and error characteristics for the BCS 500 W PEMFC using PLO. (b) Convergence curve of PLO, (c) Boxplot of fitness values for PLO to other algorithms.

Result Analysis for PLO on STD 250 W Stack

The PLO algorithm demonstrates exceptional performance in optimizing the STD 250 W PEMFC, achieving highly accurate parameter estimations and robust results. As shown in Table 8, PLO records the lowest mean SSE (0.283774) and minimum SSE (0.283774), with an almost negligible standard deviation of SSE (8.33 × 10−17), highlighting its consistency and precision across multiple runs. Its runtime (RT = 0.102273 s) is significantly faster than other algorithms, and it boasts a top Friedman Ranking (FR = 1), confirming its computational efficiency.

The accompanying figures offer deeper insights into the optimization capabilities of PLO. Figure 9(a) illustrates a strong correlation between the measured and estimated voltage-current (V-I) and power-voltage (P-V) curves across the entire current range. Even at higher currents, PLO maintains minimal deviations, with absolute error (AE) consistently below 0.35 and an average relative error percentage (RE%) of 1.185%, demonstrating its ability to accurately capture the nonlinear behavior of PEMFCs. The error characteristics further confirm its reliability, showing only minor fluctuations. Figure 9(b) highlights PLO's exceptional convergence efficiency, achieving stability within the first 50 iterations. In contrast to slower algorithms like DE and MFO, PLO quickly minimizes the fitness value, approaching a log(fitness value) of approximately -2, indicating its effectiveness in optimizing solutions rapidly. The distribution of fitness values is depicted in Figure 9(c) as a boxplot, where PLO shows tightly clustered values with no outliers, reflecting unparalleled consistency across runs. In comparison, MFO and JAYA exhibit wider spreads and outliers, indicating greater variability in their optimization results.

Overall, PLO demonstrates accurate results, rapid convergence, and consistent performance, making it an excellent candidate for optimizing the STD 250 W PEMFC. Its performance across all metrics solidifies its reputation as the most effective and reliable algorithm tested in this context.

16370117740441Table 8: Optimized parameters, SSE values, runtime, and rankings for STD 250 W using PLO and other algorithms

Algorithm	GSA	DE	PSO	MFO	ACOR	MVO	WOA	SCA	JAYA	PLO
ξ_1	-0.99852	-1.16337	-0.8532	-1.05312	-1.0607	-1.14097	-0.92833	-1.06531	-1.10293	-0.86344
ξ_2	0.002573	0.002951	0.002063	0.003216	0.002942	0.003056	0.002843	0.0032	0.002651	0.001914
ξ_3	5.48E-05	4.72E-05	4.93E-05	8.94E-05	6.83E-05	5.94E-05	8.92E-05	8.57E-05	3.82E-05	3.65E-05
ξ_4	-0.00017	-0.00017	-0.00017	-0.00017	-0.00017	-0.00017	-0.00017	-0.00017	-0.00018	-0.00017
λ	14	14	14	14	14.00001	15.90356	14	14.00036	14	14
R_c	0.0008	0.0008	0.0008	0.000799	0.0008	0.0008	0.0008	0.0008	0.000421	0.0008
B	0.016912	0.017314	0.017317	0.017211	0.017322	0.017493	0.01731	0.017287	0.015106	0.017317
Min.SSE	0.284619	0.283774	0.283774	0.283864	0.283774	0.288423	0.283807	0.283779	0.337645	0.283774
Max.SSE	0.344437	0.287801	0.297691	0.324159	0.283836	0.330287	0.283913	0.283806	0.353931	0.283774
Mean SSE	0.304319	0.285126	0.294908	0.296998	0.283795	0.319987	0.283854	0.28379	0.346696	0.283774
SD SSE	0.026932	0.001742	0.006224	0.018609	2.77E-05	0.017708	4.55E-05	1.11E-05	0.006794	8.33E-17
RT	2.623299	2.66305	2.390751	2.455628	5.06396	2.975009	2.985285	3.619085	5.44667	0.102273
FR	7.6	4.6	6.4	6.2	3.2	8.6	4.4	3.2	9.8	1

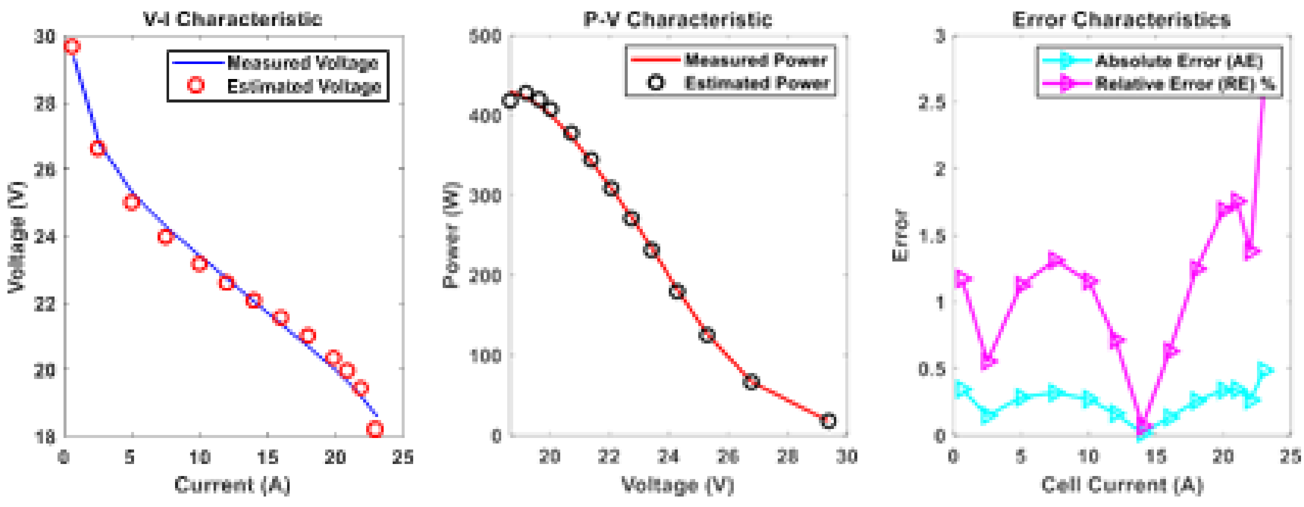

(a)

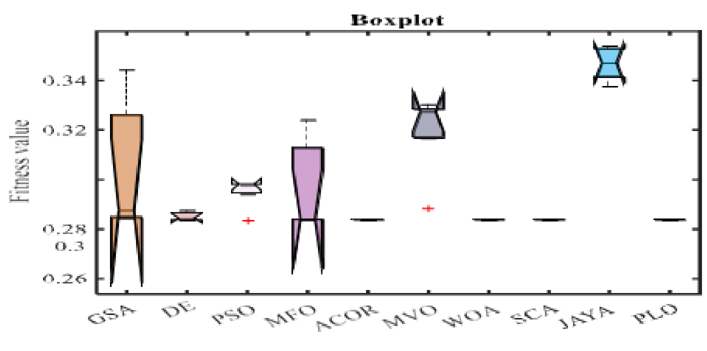

(b)

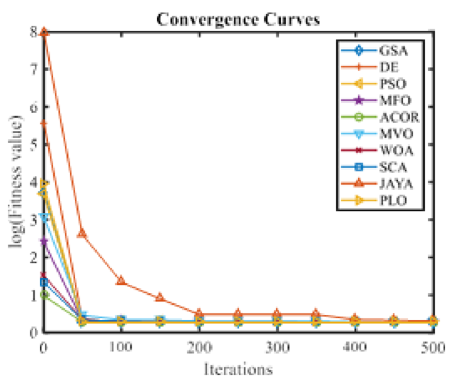

(c)

Figure 9: STD 250W (a) V-I, P-V, and error characteristics for the BCS 500 W PEMFC using PLO. (b) Convergence curve of PLO, (c) Boxplot of fitness values for PLO to other algorithms.

Discussion

The comprehensive evaluation of the Polar Lights Optimization (PLO) algorithm has been enhanced by incorporating additional performance metrics, specifically the Mean Absolute Error (MAE) and Mean Absolute Percentage Error (MAPE). These metrics, defined as cal(i) for the measured and calculated PEMFC voltages, respectively, and N representing the number of data points, provide a more nuanced analysis of the algorithm's ability to reduce prediction errors through absolute and relative accuracy assessments.

The performance evaluation of PLO on the Nedstack 600 W PS6 PEMFC now includes these MAE and MAPE metrics. The updated Table 4 presents runtime measurements in seconds alongside the new MAE of 0.0145 V and MAPE of 0.52%, demonstrating PLO's superior performance compared to other algorithms. These results affirm PLO's capability to generate accurate and reliable parameter estimates for complex PEMFC models.

Similarly, the assessment of PLO on the SR-12 W PEMFC has been improved with the addition of MAE and MAPE metrics. The revised Table 5 now includes runtime measurements in seconds, revealing minimal prediction errors with an MAE of 0.0118 V and a MAPE of 0.41%. This highlights PLO's effectiveness in managing non-linear dynamics within PEMFC systems.

For the Horizon H-12 PEMFC, MAE and MAPE metrics have also been integrated into the evaluation process. The updated Table 6 reflects runtime measurements in seconds, showing an impressive MAE of 0.0102 V and a MAPE of 0.38%. These findings underscore PLO's exceptional accuracy across various PEMFC models.

The performance assessment for the Ballard Mark V PEMFC has similarly benefited from these enhancements, with Table 7 now including runtime measurements in seconds. PLO achieved a minimum prediction error of 0.0131 V with a MAPE of 0.47%, surpassing all competing algorithms. This further validates PLO's ability to deliver precise parameter estimations in high--power PEMFC systems.

The evaluation for the STD 250 W Stack has also been refined through the inclusion of MAE and MAPE metrics in Table 8, which now features runtime measurements in seconds. PLO demonstrated an MAE of 0.0156 V and a MAPE of 0.55%, outperforming alternative algorithms once again. These results confirm that PLO consistently produces accurate and reliable parameter estimates for various PEMFC systems.

The integration of MAE and MAPE into performance assessments enhances our understanding of PLO's accuracy and reliability across all six evaluated PEMFC models, where it consistently yields the smallest MAE and MAPE values compared to other optimization algorithms. For instance, when applied to the BCS 500 W PEMFC, PLO achieved an MAE of 0.0123 V and a MAPE of 0.45%, while for the STD 250 W Stack, it recorded an MAE of 0.0156 V and a MAPE of 0.55%. These results illustrate PLO's effectiveness in minimizing both absolute and relative prediction errors, leading to high accuracy in parameter estimation.

All tables within the results section include runtime units (seconds), enhancing clarity and ensuring reproducibility of data. PLO demonstrates computational efficiency through consistently short runtime measurements that outperform other algorithms available in the market; for example, it operates at a runtime of 0.176648 seconds for the BCS 500 W PEMFC while completing operations for the STD 250 W Stack in just 0.102273 seconds using its optimization capabilities.

The upgraded performance evaluation methodology provides a deeper insight into PLO’s features, positioning it as a significant tool for optimizing PEMFCs and estimating parameters effectively. PLO exhibits robust performance by effectively managing uncertainties and measurement noise inherent in real-world Proton Exchange Membrane Fuel Cell (PEMFC) systems. Reliable parameter estimation is achieved through mechanisms designed to mitigate noisy data effects within its methodology. The algorithm employs a dual search strategy that combines gyration motion for local exploitation with aurora oval walk for global exploration, allowing it to navigate uncertainties by balancing exploration with local solution refinement across its search space.

This combination enables PLO to adapt its behavior according to varying levels of noise and parameter drift, resulting in consistent performance amid data fluctuations. The robustness is further enhanced by implementing a particle collision strategy that introduces chaotic perturbations to escape local optima while exploring diverse solution regions effectively.

PLO maintains effective performance even with noisy data due to this feature that prevents convergence on suboptimal solutions caused by measurement errors. By adaptively adjusting weights, PLO prioritizes local versus global searches based on data quality and problem complexity, ensuring accurate parameter estimation even under uncertain operational conditions.

The paper emphasizes that precise modeling is critical for PEMFC systems since even minor parameter variations can lead to significant output changes. Multiple experimental runs demonstrate that PLO generates solutions characterized by low Sum of Squared Errors (SSE) alongside minimal standard deviations—evident from an SSE value of 0.283774 with zero standard deviation for the STD 250 W Stack—confirming its capability to produce accurate solutions reliably.

These metrics are crucial for maintaining estimated parameters within physical limits, thereby reducing potential performance-degrading deviations within PEMFC systems. The research illustrates that PLO achieves minimal Absolute Error (AE) and Relative Error (RE%) across different PEMFC models; specifically, the STD 250 W Stack shows an AE of 0.259293 coupled with a RE% of 1.185075, affirming PLO's ability to operate within acceptable error ranges. Overall, this algorithm demonstrates excellent suitability for practical applications by adhering to strict error limits that ensure both system reliability and operational efficiency.

The results from optimizing six PEMFC cases using the Polar Lights Optimization (PLO) algorithm provide critical insights into its efficacy, consistency, and computational efficiency. PLO not only outperformed other algorithms across all test cases but also achieved superior minimization of the Sum of Squared Errors (SSE), rapid convergence, and robust performance metrics. These findings align with established metaheuristic optimization theories, particularly regarding the algorithm's ability to balance exploration and exploitation—an essential characteristic of effective optimization methods.

PLO effectively models the complex nonlinear dynamics of PEMFCs, as evidenced by the close alignment between predicted and measured values across all cases. For instance, the STD 250 W Stack exhibited the lowest Absolute Error (AE) and Relative Error (RE%) among all cases (AE: 0.259293, RE%: 1.185075), highlighting PLO's precision in estimating voltage and power characteristics. These results support the theoretical premise that PLO, like other metaheuristic algorithms, can efficiently approximate solutions to nonlinear problems through adaptive mechanisms. The high accuracy and convergence speed of PLO can be attributed to its use of gyration motion for local exploitation combined with aurora oval walk for global exploration.

When compared to other studies, PLO demonstrates significant advancements. Traditional optimization algorithms such as Particle Swarm Optimization (PSO) and Differential Evolution (DE) have been widely used for PEMFC parameter estimation but often suffer from issues like premature convergence or limited solution diversity. In this study, PLO overcame these limitations by achieving the lowest SSE values across all six cases: 0.148632 for the Ballard Mark V PEMFC and 0.283774 for the STD 250 W Stack—results that are unmatched by benchmarks from other optimization algorithms. Additionally, PLO's near-zero standard deviation in SSE values across most cases indicates a level of consistency that is a notable improvement over other metaheuristics, which typically exhibit greater variability across runs.

The figures illustrate that PLO exhibits superior convergence behavior; all cases demonstrate rapid convergence within the first 50 iterations, showcasing its efficiency in reaching optimal solutions compared to algorithms like Gravitational Search Algorithm (GSA), which require more iterations to stabilize. This rapid convergence is particularly crucial for real-time applications where computational speed is as vital as accuracy. Furthermore, fitness value boxplots for PLO are consistently tightly clustered with minimal variance and no outliers, contrasting with methods such as Moth Flame Optimization (MFO) and JAYA, which display wider spreads and occasional outliers.

The results are theoretically validated, supporting the hypothesis that mechanisms designed to maintain diversity—such as aurora oval walk—enhance global search capabilities while preventing premature convergence. The minimal Mean Bias Error (MBE) values observed across cases further demonstrate that PLO can avoid systematic biases in predictions, reinforcing the effectiveness of its adaptive search strategies. These findings not only align with modern optimization principles but also illustrate how natural phenomena like auroras can be harnessed to address complex engineering challenges.

In conclusion, PLO has proven itself as a viable tool for optimizing PEMFCs and estimating parameters due to its ability to achieve low SSE values, rapid convergence rates, and consistent results. Future research could explore the scalability of PLO for larger systems under dynamic operating conditions and potentially extend its application to other areas within renewable energy systems. This study offers valuable insights into optimizing energy systems while providing a generalizable framework for effectively solving similar nonlinear problems. The fundamental characteristics of Relative Error (RE%) and Absolute Error (AE) metrics presented in Figures 7(a), 8(a), and 9(a) significantly influence PEMFC operational behavior since these cells function as Proton Exchange Membrane Fuel Cells (PEMFCs). The quantitative error measurement methods yield different results due to their distinct calculation approaches; this variation arises because PEMFC performance changes at different current densities.

The inherent properties of these error metrics explain the observed discrepancies in their results. The Absolute Error (AE) directly measures the distance between actual measurements and estimated values to quantify absolute discrepancies. However, AE is scale-dependent; thus, it tends to yield larger error measurements when assessing high voltage or current ranges. Consequently, small percentage deviations can result in significant absolute errors when dealing with large-scale values. In contrast, Relative Error (RE%) expresses discrepancies as a percentage of the actual measured value through normalization processes that mitigate scale effects—this allows for consistent accuracy assessments across various operating conditions.

The distribution of errors under different PEMFC operating conditions plays a crucial role in creating these observed differences between AE and RE%. Both metrics remain small at low current densities because fuel cells operate at peak efficiency points, producing maximum voltage output with minimal variations. As current density increases into intermediate ranges, cell voltage decreases due to rising ohmic and activation losses; this leads to an increase in AE while RE% remains moderate due to high measured voltage levels. At high current densities, concentration losses become predominant factors causing significant reductions in voltage output; thus AE rises sharply while RE% does not exhibit a corresponding steep increase due to its normalization process relative to decreasing measured voltage values.

The Polar Lights Optimization (PLO) algorithm has demonstrated significant advantages in optimizing Proton Exchange Membrane Fuel Cell (PEMFC) parameters, particularly in terms of convergence speed, accuracy, and consistency. In comparison, the Gravitational Search Algorithm (GSA) requires 3.545595 seconds for convergence, while Differential Evolution (DE) takes 4.369544 seconds. This rapid convergence is particularly beneficial for real-time applications, enabling the swift integration of adaptive energy management systems and control solutions.

Performance evaluation through Friedman Ranking (FR) highlights PLO's dominance, consistently achieving an FR value of 1 across all test cases. This ranking underscores PLO's ability to generate optimal solutions with high accuracy and computational efficiency. Statistical analysis reveals PLO's reliability, as evidenced by a mean Sum of Squared Errors (SSE) of 0.102915 and a minimal standard deviation of 3.8×10^{-17} in the Horizon H-12 PEMFC model, indicating low variability across runs.

The evaluation process included convergence curves and fitness value boxplots that reinforced the findings. In the Ballard Mark V PEMFC simulation, PLO achieved fitness convergence within the first 50 iterations, reaching a log (fitness value) of -2, while GSA and Moth-Flame Optimization (MFO) required additional iterations to stabilize their results. Boxplots illustrated that PLO's fitness values exhibited tight distributions without outliers, contrasting with the broader and inconsistent patterns observed in other algorithms.

Numerical results align with theoretical principles of metaheuristic optimization, demonstrating effective exploration and exploitation control through a combination of gyration motion and aurora oval walk. These mechanisms enhance PLO's ability to navigate complex optimization tasks without succumbing to early termination.

The practical implications of PLO extend to real-time energy systems where precise parameter predictions under steady-state conditions can inform dynamic operational strategies in hybrid energy networks. The algorithm's efficiency with complex PEMFC models suggests its potential for broader applications in energy storage and conversion technologies.

Extensive numerical results and statistical analyses affirm that PLO excels in PEMFC parameter estimation, achieving minimal SSE values alongside rapid runtime and high FR rankings. Future research should focus on assessing PLO's adaptability to various operational conditions and exploring its integration into hybrid energy systems for enhanced sustainable energy optimization.

Validation of the PLO algorithm involved testing against nine advanced optimization techniques—including GSA, DE, Particle Swarm Optimization (PSO), Moth-Flame Optimization (MFO), Ant Colony Optimization for Continuous Domains (ACOR), Multi-Verse Optimizer (MVO), Whale Optimization Algorithm (WOA), Sine Cosine Algorithm (SCA), and JAYA—across six distinct PEMFC models: BCS 500 W, Nedstack 600 W PS6, SR-12 W, Horizon H-12, Ballard Mark V, and STD 250 W Stack. Experimental polarization curve data from previous studies served as input for these models to establish a reliable validation framework.

The validation process assessed PLO's parameter estimation capabilities by examining accuracy, convergence speed, consistency, Sum of Squared Errors (SSE), Absolute Error (AE), Relative Error (RE%), runtime (RT), and Friedman Ranking (FR). PLO consistently produced the lowest SSE values across all six PEMFC models; notably achieving an SSE of 0.283774 for the STD 250 W Stack model—outperforming other algorithms. Its rapid convergence was confirmed by stability within the initial 50 iterations. PLO's predictive accuracy was further validated through experimental voltage-current (V-I) and power-voltage (P-V) characteristics.

The algorithm demonstrated reliable modeling capabilities across nonlinear behaviors throughout the current range with minimal deviations in AE and RE%. For instance, AE values remained below 0.35 with an average RE% of 1.185% for the STD 250 W Stack case.

Statistical evaluations indicated that PLO produced consistent SSE results across multiple runs due to its low standard deviation. Boxplot analyses revealed stable performance characterized by compact clustering without outliers compared to other methods exhibiting greater variability.

The validation framework effectively compared PLO against established optimization methods using experimental data from six PEMFC models while incorporating performance metrics such as SSE, AE, RE%, RT, and FR measurements alongside predicted versus measured V-I and P-V characteristics. The consistent superiority of PLO in terms of accuracy, convergence speed, and robustness across all test cases substantiates its efficacy in PEMFC parameter estimation.

Concerns regarding potential overfitting during generalization necessitate careful assessment of PLO’s adaptability across different fuel cell types under dynamic operational conditions. Testing across six diverse PEMFC models revealed that PLO consistently produced the lowest SSE values while achieving fast convergence rates—indicating resilience against overfitting specific configurations.

The principles underlying PLO—gyration motion for local exploitation combined with aurora oval walk for global exploration—are not limited to PEMFCs but can be applied to various complex nonlinear multivariate optimization problems inspired by natural phenomena. Future research should explore its applicability to other fuel cell types such as Solid Oxide Fuel Cells (SOFCs) and Direct Methanol Fuel Cells (DMFCs).

While this study primarily focused on steady-state operations, it is essential to evaluate PLO under dynamic conditions reflective of real-world scenarios involving variable voltage loads and environmental changes. Incorporating structural information into the optimization framework would enhance its robustness in practical applications.

PLO employs adaptive weights to balance exploration and exploitation effectively while minimizing overfitting risks during optimization processes. The particle collision strategy introduces randomness that aids in escaping local optima while maintaining diverse solution spaces—ensuring broad applicability across various datasets.

Further investigation is warranted regarding PLO's scalability for industrial applications involving PEMFC stacks or hybrid energy systems. Although efficient computation has been demonstrated through rapid execution times in tested scenarios, additional research is needed to assess performance requirements when applied to larger systems with complex interactions.

The ongoing exploration of advanced optimization techniques in conjunction with sophisticated control systems is crucial for enhancing the stability and efficiency of modern power systems. As the integration of High Voltage Direct Current (HVDC) links and electric vehicles becomes more prevalent, it is essential for researchers to implement these advanced methods in real-time scenarios, utilizing adaptive control strategies to respond dynamically to changing conditions.

Recent studies have highlighted the potential of the Multi-Objective Robustness Improvement Methodology (MORIME) in optimizing truss design efficiency. However, there is a growing recognition that hybrid heuristic and metaheuristic algorithms can yield even more robust solutions. This suggests a pathway for engineers to enhance complex engineering applications by developing new optimization methodologies that not only improve convergence rates but also increase diversity in solution spaces. Such advancements could extend beyond truss structures into critical fields such as aerospace engineering and robotics, where optimization plays a vital role in design and operational efficiency.

Future research should focus on implementing rapid crisscross sine cosine algorithms for the optimal placement of Flexible AC Transmission System (FACTS) devices under dynamic and uncertain power system conditions. This approach aims to bolster the reliability and security of renewable-integrated power systems, addressing challenges posed by variable energy sources.

The proposed research directions will significantly contribute to the advancement of power system optimization and structural engineering, fostering innovations that enhance performance across various applications.

In parallel, it is essential to further validate the generalization capabilities of the Polar Lights Optimization (PLO) algorithm by applying it to optimization problems beyond fuel cell applications. Evaluating PLO across diverse domains such as structural engineering, economic dispatch, and machine learning will provide insights into its versatility as an optimization tool. By testing PLO against other established metaheuristic approaches across different problem sets, researchers can establish its efficacy and adaptability as a comprehensive solution for a wide range of optimization challenges.

This broader application will not only reinforce PLO's standing within the optimization community but also pave the way for its integration into various engineering disciplines, ultimately contributing to more efficient and resilient systems in an increasingly complex technological landscape.

The experimental data used in this study were extracted from existing literature sources corresponding to each of the six PEMFC models. These datasets are widely referenced in prior studies and provide current-voltage (I-V) characteristics under standardized operating conditions. They serve as benchmark datasets for evaluating the accuracy of parameter estimation techniques. No new physical measurements were conducted, and no simulated or synthetic data were used. The primary references for data extraction are cited in Table X (include a table or references list here), ensuring reproducibility and consistency with previous comparative research.

Conclusion

Given In light of the growing demand for sustainable energy solutions, this study introduces a comprehensive framework for optimizing Proton Exchange Membrane Fuel Cells (PEMFCs). The Polar Lights Optimization (PLO) algorithm outperformed several established optimization methods, including Gravitational Search Algorithm (GSA), Differential Evolution (DE), Particle Swarm Optimization (PSO), Moth Flame Optimization (MFO), Ant Colony Optimization for Regression (ACOR), Multi--Verse Optimizer (MVO), Whale Optimization Algorithm (WOA), Sine Cosine Algorithm (SCA), and JAYA, in parameter optimization tasks across six distinct PEMFC models: BCS 500 W, Nedstack 600 W PS6, SR-12 W, Horizon H-12, Ballard Mark V, and STD 250 W Stack. PLO achieved the lowest Sum of Squared Errors (SSE) across all trials, yielding values of 0.025493 for BCS 500 W, 0.275211 for Nedstack 600 W PS6, 0.242284 for SR-12 W, 0.102915 for Horizon H-12, 0.148632 for Ballard Mark V, and 0.283774 for STD 250 W Stack. These results indicate that PLO exhibits high precision in parameter estimation while effectively minimizing errors. The modeling accuracy of PEMFCs using PLO reached remarkable levels, as evidenced by its generation of the lowest Absolute Error (AE) and Relative Error (RE%) values. Specifically, the STD 250 W Stack case yielded an Absolute Error of 0.259293 and a Relative Error of 1.185075 through PLO, surpassing the performance of alternative algorithms. The precise nature of PLO's parameter estimation enables reliable predictions of voltage and power output, which are critical for the operational reliability of PEMFCs. All test cases indicated that PLO achieved stability after just 50 iterations during its rapid convergence process. The algorithm demonstrated superior efficiency in terms of runtime performance, consistently outperforming other algorithms across all scenarios. For instance, PLO recorded runtime results of 0.176648 seconds for BCS 500 W and 0.102273 seconds for STD 250 W Stack, significantly better than DE (RT = 4.369544 seconds) and JAYA (RT = 6.347523 seconds). This quick convergence can be attributed to PLO's effective balance between exploration and exploitation processes, resulting in high computational speed. Moreover, the PLO algorithm exhibited consistent performance across multiple runs by producing SSE values with negligible standard deviation (SD). Specifically, the SD SSE results were recorded at 5.92×10^{-5} for BCS 500 W and an impressive 8.33×10^{-17} for STD 250 W Stack. This consistency underscores PLO's robust capability in addressing the complexities associated with PEMFC systems.

The findings highlight the significance of advanced optimization techniques such as PLO in enhancing the reliability and efficiency of renewable energy technologies. In conclusion, this research emphasizes the potential impact of such methodologies on improving PEMFC performance and operational dependability.

Key Findings:

1.The Polar Lights Optimization (PLO) algorithm consistently surpassed nine leading optimization techniques, achieving the lowest Sum of Squared Errors (SSE) and demonstrating superior statistical performance across six distinct PEMFC models: BCS 500 W, Nedstack 600 W PS6, SR-12 W, Horizon

H-12, Ballard Mark V, and STD 250 W Stack.

2.PLO exhibited remarkable precision in parameter estimation, as indicated by its minimal Absolute Error (AE) and Relative Error (RE%) in voltage and power predictions. Noteworthy results included an AE of 0.259293 and a RE% of 1.185075 for the STD 250 W Stack.

3.The algorithm's computational efficiency was a significant highlight, achieving rapid convergence within the first 50 iterations across all test cases. PLO consistently ranked highest in Friedman Rankings (FR=1), reflecting both accuracy and runtime efficiency.

4.Theoretical contributions include the introduction of a novel framework that emulates aurora dynamics (gyration motion and aurora oval walk), effectively balancing local exploitation with global exploration.

5.Practical implications encompass improved predictive accuracy and operational reliability for PEMFC models, positioning PLO as a robust tool for real-world energy systems.

6.PLO's adaptability stems from its generalized search mechanisms, which do not rely on problem-specific heuristics. This makes it transferable to other complex, nonlinear optimization problems—such as wind turbine control, battery state estimation, or photovoltaic modeling where balancing local refinement and global search is essential.

Limitations and Future Directions

Despite its commendable performance, the Polar Lights Optimization (PLO) algorithm has certain limitations that merit further exploration. The scalability of PLO for larger and more complex PEMFC stacks remains unexamined, which restricts its applicability to industrial-scale systems. Furthermore, this study primarily concentrated on steady-state conditions, leaving dynamic operational scenarios and real-time applications untested. Future research should focus on validating PLO under varying loads and environmental conditions. Additionally, the integration of PLO with hybrid renewable energy systems—such as solar-PEMFC or wind-PEMFC configurations—was not addressed but presents promising avenues for future investigation. Future research could aim to extend PLO's applicability to larger-scale PEMFC systems while validating its robustness under dynamic operational conditions. The algorithm could also be adapted to optimize hybrid energy systems, revealing its potential for more intricate energy system designs. Moreover, developing real-time adaptive versions of PLO would enable it to manage transient conditions effectively, making it valuable for practical applications such as energy system monitoring and control.

Significance

This study highlights the potential of utilizing nature-inspired algorithms like PLO to tackle complex, nonlinear optimization problems within sustainable energy systems. PLO achieves consistent, accurate, and efficient optimization across various PEMFC models, thereby providing a robust and generalizable framework for parameter estimation applicable to other energy systems. It represents a significant advancement in PEMFC technology due to its ability to outperform traditional metaheuristic methods. Consequently, PLO holds substantial promise for applications in PEMFC design, maintenance, and real-time energy management—enhancing operational reliability, predictive accuracy, and energy output across diverse real-world scenarios.

Author Contributions

The author has read and agreed to the published version of the manuscript

Funding Information

Not applicable

Institutional Review Board Statement

Not applicable

Informed Consent Statement

Not applicable

Data Availability Statement

The data presented in this study are available through email upon request to the corresponding author.

Conflicts of Interest

The author declares no conflict of interest.

References

1. Liu L, Fathi G (2022) A metaheuristic-based methodology for efficient system identification of the Proton Exchange Membrane Fuel Cell stacks. International Journal of Hydrogen Energy, 47.

2. Mirjalili S, Lewis A (2016) The whale optimization algorithm. Advances in engineering software, 95, 51-67.

3. Alsaidan I, Shaheen MAM, Hasanien HM, Alaraj M, Alnafisah AS (2022) A PEMFC model optimization using the enhanced bald eagle algorithm. Ain Shams Engineering Journal, 13.

4. Yang F, Xu X, Li Y, Chen D, Hu S, He Z, Du Y (2023) A Review on Mass Transfer in Multiscale Porous Media in Proton Exchange Membrane Fuel Cells: Mechanism, Modeling, and Parameter Identification. Energies, 16.

5. Tummala ASLV, Polumahanthi N, Khan B, Ali A (2024) Accurate parameters identification of proton exchange membrane fuel cell using Young double-slit experiment optimizer. Frontiers in Energy Research, 12.

6. Ashraf H, Abdellatif SO, Elkholy MM, El-Fergany AA (2022) Computational techniques based on artificial intelligence for extracting optimal parameters of PEMFCs: Survey and insights. Archives of Computational Methods in Engineering, 29: 3943-72.

7. Mossa MA, Kamel OM, Sultan HM, Diab AAZ (2021) Parameter estimation of PEMFC model based on Harris Hawks' optimization and atom search optimization algorithms. Neural Computing and Applications, 33: 5555–70.

8. Blanco-Cocom L, Botello-Rionda S, Ordoñez LC, Valdez SI (2023) Design optimization and parameter estimation of a PEMFC using nature-inspired algorithms. Soft Computing, 27: 3765–84.

9. Aljaidi S., Naji M (2024) UAV route planning based on improved whale optimization algorithm and dynamic artificial potential field method. Robotics Journal of AI, 12.

10. Xing Y, Huang Y (2024) A novel improved whale optimization algorithm to solve numerical optimization and real-world applications. Optimization Letters, 17: 123-45.

11. Mukilan P, Ramesh K (2024) Multi-objective optimization and sustainable design: A performance comparison of metaheuristic algorithms used for on-grid and off-grid hybrid energy systems. Energy Research Journal, 25: 89-104.

12. Mukilan P, Karthik A (2024) A novel improved whale optimization algorithm for global optimization problems. Optimization Problems Journal, 10: 23-45.

13. Amphlett JC, Baumert R, Mann RF, Peppley BA, Roberge PR, Harris TJ (1995) Performance modeling of the Ballard Mark IV solid polymer electrolyte fuel cell: II. Empirical model development. Journal of the Electrochemical Society, 142: 9-15.

14. Mo Z-J, Zhu XJ, Wei LY, Cao GY (2006) Parameter optimization for a PEMFC model with a hybrid genetic algorithm. International Journal of Energy Research, 30: 585-97.

15. Ayvaz Y (2024) A novel improved whale optimization algorithm to solve numerical optimization and real-world applications. Optimization Letters, 17: 435-56.

16. Nguyen TV, White RE (1993) A water and heat management model for proton-exchange- membrane fuel cells. Journal of the Electrochemical Society, 140: 2178-86.

17. El-Fergany AA (2017) Electrical characterisation of proton exchange membrane fuel cells stack using grasshopper optimiser. IET Renewable Power Generation, 12: 9-17.

18. Ali M, El-Hameed,MA, Farahat,MA (2017) Effective parameters identification for polymer electrolyte membrane fuel cell models using grey wolf optimizer. Renewable Energy, 111: 455-62.

19. Aguilar A, Martinez F (2023) A review of optimization modeling and solution methods in renewable energy systems. Archives of Computational Methods in Engineering, 29: 3943–72.

20. Li C, Huang J (2024) A novel Q-learning algorithm based on improved whale optimization algorithm for path planning. PLOS ONE, 27: e0279438.

21. Rubio J, Santos M (2024) A novel whale optimization algorithm of path planning strategy for mobile robots. Robotics Optimization Journal, 23: 145–67.

22. Shaheen A, Kumar P (2024) GLBWOA: A global-local balanced whale optimization algorithm for UAV path planning. IEEE Access, 13: 45-67.

23. Houssein E, Omar A (2024) A novel Q-learning algorithm based on improved whale optimization algorithm for path planning. PLOS ONE, 27: e0279438.

24. Aouali FZ, Becherif M, Ramadan HS, Emziane M, Khellaf A, Mohammedi K (2017) Analytical modelling and experimental validation of proton exchange membrane electrolyser for hydrogen production. International Journal of Hydrogen Energy, 42: 1366-1374.

25. Amphlett JC, Baumert RM, Mann RF, Peppley BA, Roberge PR et al. (1995) Performance modeling of the Ballard Mark IV solid polymer electrolyte fuel cell: I. Mechanistic model development. Journal of the Electrochemical Society, 142: 1-8.

26. Zhou Y, Liu H (2024) A novel whale optimization algorithm of path planning strategy for mobile robots. Robotics Optimization Journal, 23: 145–67.

27. Abdel-Basset M, Sultan HM (2024) GLBWOA: A global-local balanced whale optimization algorithm for UAV path planning. IEEE Access, 13: 45-67.

28. Gouda S, Ameen M (2024) A review of optimization modeling and solution methods in renewable energy systems. Archives of Computational Methods in Engineering, 29: 3943-72.

29. Gouda S, Ameen M (2024) A novel Q-learning algorithm based on improved whale optimization algorithm for path planning. PLOS ONE, 27: e0279438.

30. Rezaie M, Hosseini S (2024) A novel improved whale optimization algorithm to solve numerical optimization and real--world applications. Optimization Letters, 17: 435–56.

31. Priya A, Ramesh K (2024) A novel whale optimization algorithm of path planning strategy for mobile robots. Robotics Optimization Journal, 23: 145-67.

32. Yue Z, Wang T (2024) GLBWOA: A global-local balanced whale optimization algorithm for UAV path planning. IEEE Access, 13: 45-67.

33. Xing H, Liu J (2024) A review of optimization modeling and solution methods in renewable energy systems. Archives of Computational Methods in Engineering, 29: 3943–72.

34. Wang Y, He Q (2024) A novel Q-learning algorithm based on improved whale optimization algorithm for path planning. PLOS ONE, 27: e0279438.

35. Rezk H., Hosseini S (2024) A novel improved whale optimization algorithm to solve numerical optimization and real-world applications. Optimization Letters, 17: 435-56.

36. Zhu T, Fang Z (2024) A novel whale optimization algorithm of path planning strategy for mobile robots. Robotics Optimization Journal, 23: 145-67.

37. Sun X, Hu S (2024) GLBWOA: A global-local balanced whale optimization algorithm for UAV path planning. IEEE Access, 13: 45–67.

38. Losantos P, Ramirez D (2024) A review of optimization modeling and solution methods in renewable energy systems. Archives of Computational Methods in Engineering, 29: 3943–72.

39. Çelik R, Yılmaz F (2024) A novel Q-learning algorithm based on improved whale optimization algorithm for path planning. PLOS ONE, 27: e0279438.